

2014-01-01

# A Robust Algorithm For Estimating The Balance Of Autonomic Nervous System With Application To Mental Fatigue Detection Using Photoplethysmographic (ppg) Signals

Ajay Kumar Verma

University of Texas at El Paso, akverma7@outlook.com

Follow this and additional works at: [https://digitalcommons.utep.edu/open\\_etd](https://digitalcommons.utep.edu/open_etd)



Part of the [Electrical and Electronics Commons](#)

---

## Recommended Citation

Verma, Ajay Kumar, "A Robust Algorithm For Estimating The Balance Of Autonomic Nervous System With Application To Mental Fatigue Detection Using Photoplethysmographic (ppg) Signals" (2014). *Open Access Theses & Dissertations*. 1756.  
[https://digitalcommons.utep.edu/open\\_etd/1756](https://digitalcommons.utep.edu/open_etd/1756)

This is brought to you for free and open access by DigitalCommons@UTEP. It has been accepted for inclusion in Open Access Theses & Dissertations by an authorized administrator of DigitalCommons@UTEP. For more information, please contact [lweber@utep.edu](mailto:lweber@utep.edu).

A ROBUST ALGORITHM FOR ESTIMATING THE BALANCE OF  
AUTONOMIC NERVOUS SYSTEM WITH APPLICATION TO MENTAL  
FATIGUE DETECTION USING PHOTOPLETHYSMOGRAPHIC (PPG)  
SIGNALS

AJAY KUMAR VERMA

Department of Electrical and Computer Engineering

APPROVED:

---

Sergio D Cabrera, Ph.D., Chair

---

Homer Nazeran, Ph.D.

---

Tzu-Liang (Bill) Tseng, Ph.D.

---

Bess Sirmon-Taylor, Ph.D.  
Interim Dean of the Graduate School

Copyright ©

by

Ajay K Verma

2014

## DEDICATION

To my grandmother *late Rajvanti Devi*

A ROBUST ALGORITHM FOR ESTIMATING THE BALANCE OF  
AUTONOMIC NERVOUS SYSTEM WITH APPLICATION TO MENTAL  
FATIGUE DETECTION USING PHOTOPLETHYSMOGRAPHIC (PPG)  
SIGNALS

by

AJAY KUMAR VERMA, Bachelor of Technology

THESIS

Presented to the Faculty of the Graduate School of

The University of Texas at El Paso

in Partial Fulfillment

of the Requirements

for the Degree of

MASTER OF SCIENCE

Department of Electrical and Computer Engineering

THE UNIVERSITY OF TEXAS AT EL PASO

May 2014

## ACKNOWLEDGEMENTS

I would like to thank my thesis advisor and committee chair Dr. Sergio Cabrera for guiding me through my master's thesis. His guidance was really important especially during the early phase of this research when I had very little experience doing research in this area. His direction whether it was related to research or choosing right courses during course work period helped me to develop a positive attitude towards research work and better prepared me to further my education to a doctorate level after completing master's degree in Electrical Engineering. I would also like to thank Dr. Cabrera for providing me financial support for travel expenses for attending a conference to present my research and for buying equipments needed for research.

I would like to thank *Texas Instruments Foundation Endowed Scholarship* Program for providing me financial support to pursue a master's degree in Electrical Engineering at The University of Texas at El Paso.

I would like to thank Dr. Nazeran my thesis committee Co-Chair for his valuable suggestions and help with this research; for providing me an access to his Biomedical Engineering Laboratory to use equipments throughout this research period. I would also like to thank him for providing me financial support for travel expenses to attend a conference. I would also like to thank my thesis committee member Dr. Tseng for his suggestions to improve this thesis.

Finally I would like to thank my parents for their great encouragement and support both emotionally and financially, I also thank my family and friends for their support throughout this program. This research wouldn't have been possible without their support.

## ABSTRACT

Spectral- and time-domain analysis of Heart Rate Variability (HRV) signal is widely used as a quantitative marker of the Autonomic Nervous System (ANS) activity. A robust algorithm was developed to derive HRV from photoplethysmographic (PPG) signals, to compute FFT- and AR-based spectra of these HRV signals, and to determine time- and frequency-domain features. This algorithm has detrending, sample-rate reductions, false-peak removal, automatic peak detection, peak-to-peak (P-P) interval detection and correction, time-domain feature extraction, HRV signal generation, and spectral-domain feature extraction from the HRV signal. Adapting to the very low spectral contents of the input PPG signal is very helpful in reducing the processing/computational effort. The spectral features include the LF/HF ratio since this can be used to quantify parasympathetic influences and sympathovagal balance. To validate the efficacy of the algorithm, PPG signals were recorded under different conditions such as stimulating an acupuncture point using a nanoscale patch, measuring relaxation after exercising, and others which are known to elicit changes in the state of the ANS. Significant differences in LF/HF were observed due to these effects. The pNN50, a time-domain measure of PP interval variability, was also considered for quantifying ANS activity and exploring its correlation with spectral features. We also used multiple sensors placed on different fingers to record PPG signals and to confirm that their respective spectral analysis was almost identical. We observed that a multiple sensor approach could be used to effectively reduce the impact of motion artifacts and of deterioration of signal quality due to loss of good PPG sensor contact. Finally, a time varying approach for analysis of HRV signal spectra was developed. It is proposed as a tool to estimate the ANS balance at any particular instant of time.

## TABLE OF CONTENTS

ACKNOWLEDGEMENTS .....	v
ABSTRACT.....	vi
TABLE OF CONTENTS.....	vii
LIST OF FIGURES .....	x
LIST OF TABLES .....	xiv
CHAPTER 1: INTRODUCTION.....	1
1.1 Objective.....	1
1.2 Background .....	1
1.2.1 Heart Rate Variability .....	1
1.2.2 Electrocardiography .....	2
1.2.3 Photoplethysmography .....	3
1.2.4 Autonomic Nervous System .....	4
1.2.5 Time Domain Analysis .....	6
1.2.6 Frequency Domain Analysis.....	7
1.3 Motivation.....	8
CHAPTER 2: LITERATURE REVIEW .....	10
2.1 Heart Rate Variability .....	10
2.2 HRV Derivation.....	11
2.3 Autonomic Nervous System .....	12
2.4 HRV Analysis .....	14
2.5 Data Collection .....	18
2.6 Peak Detection and HRV Derivation.....	19
2.7 Correlation Between Time and Frequency Domain Analysis .....	21
2.8 Existing HRV Analysis Software .....	22
2.9 Accuracy of PSD Based Estimation .....	24
2.10 Principal Dynamic Mode .....	24
2.11 Effects of Light on ANS .....	25
CHAPTER 3: ALGORITHM FEATURES .....	26
3.1 Data Collection .....	26

3.1.1 Multiple Sensor Concept.....	26
3.2 Sampling Rate Reduction .....	29
3.3 Preprocessing .....	32
3.4 Thresholding and Peak Detection .....	36
3.4.1 Global Threshold .....	37
3.4.2 Variable Threshold .....	38
3.5 Peak-Peak Interval Detection .....	39
3.6 P-P Outliers (Missed Peak) Detection and Correction Scheme.....	39
3.7 Heart Rate Variability Signal Derivation .....	42
3.8 Downsampling HRV Signal .....	48
3.9 Frequency Domain Analysis.....	50
3.9.1 Non-Parametric Method .....	51
3.9.2 Parametric Method.....	53
CHAPTER 4: TIME DOMAIN ANALYSIS .....	56
4.1 Time Domain Analysis .....	56
4.1.1 Long Term recording .....	56
4.1.2 Short term recording .....	56
4.2 Time Domain Analysis on Relaxed Subject.....	57
4.3 Time Domain Analysis on Normal Subject.....	59
4.4 Time Domain Analysis on Stressed Subject.....	62
CHAPTER 5: FREQUENCY DOMAIN ANALYSIS AND ALGORITHM VALIDATION .....	65
5.1 Nano-Scale Patch.....	65
5.2 Normal Condition .....	70
5.3 Blue Light Effect .....	73
CHAPTER 6: ADVANCED TECHNIQUES, CONCLUSIONS AND FUTURE WORK .....	76
6.1 A Time Varying Approach .....	76
6.1.1 Block Diagram of Time Varying Approach .....	77
6.1.2 Verification of Time Varying Analysis Algorithm .....	82
6.2 Conclusions.....	84
6.3 Future Work.....	85
6.3.1 Multiple Sensor Concept .....	85
6.3.2 More Experiments .....	85

6.3.3	HRV Analysis Using Principal Dynamic Modes .....	85
REFERENCES	.....	87
CURRICULUM VITAE	.....	90

## LIST OF FIGURES

Figure 1.1: Example of R-R intervals in a ECG signal.....	2
Figure 1.2: Example of P-P intervals in a PPG Signal. ....	3
Figure 1.3: Example of Autonomic Nervous System Regulating Functioning of Organs. ....	5
Figure 1.4: Power Spectral Density of a HRV signal. ....	8
Figure 1.5: Overall Block Diagram of Algorithm Processing. ....	9
Figure 2.1: A Typical Electrocardiogram Signal. ....	11
Figure 2.2: Various Time Domain Parameters. ....	15
Figure 2.3: Spectral Regions of Typical Power Spectral Density. ....	17
Figure 2.4: Various Frequency Domain Parameters (Long Term vs. Short Term). ....	18
Figure 2.5: Typical Signal Processing Steps.....	20
Figure 2.6: Expected Time and Frequency Domain Correlation. ....	21
Figure 2.7: KUBIOS HRV Analysis Report.....	23
Figure 3.1: A PPG Signal Collected Using Sensor 1 after Detrending. ....	27
Figure 3.2: A PPG Signal Collected Using Sensor 2 after Detrending. ....	27
Figure 3.3: A PPG Signal Collected Using Sensor 3 after Detrending. ....	28
Figure 3.4: Combined PPG Signal Using Averaging Technique. ....	28
Figure 3.5: Full Spectrum of Original Signal Sampled at 1000 Hz.....	30
Figure 3.6: PSD of a Signal Sampled at 1000 Hz.....	31
Figure 3.7: PSD of a Signal Sampled at 100 Hz.....	31
Figure 3.8: Preprocessing Steps.....	32
Figure 3.9: Pole-Zero and Frequency Response of IIR High Pass Filter.....	34
Figure 3.10: Original Signal. ....	35

Figure 3.11: Preprocessed Signal Using IIR High Pass Notch Filter. ....	35
Figure 3.12: Signal After Clipping Negative and Squaring Positive part.....	36
Figure 3.13: Determined Locations of Peaks Using Zero Crossings of Derivatives. ....	37
Figure 3.14: Variable Thresholding.....	38
Figure 3.15: Signal with Missed Peaks.....	40
Figure 3.16: Corrected Signal Using Moving Average Filter.....	40
Figure 3.17: Histogram of Peak to Peak Intervals Signal.....	41
Figure 3.18: Histogram of Heart Rate.....	42
Figure 3.19: HRV Signal Derived Using Interpolation Technique. ....	43
Figure 3.20: Example of HRV Derivation Using Nearest Method.....	44
Figure 3.21: Example of HRV Derivation Using Cubic Spline Method. ....	45
Figure 3.22: Spectrum of HRV Using Cubic Spline Method. ....	46
Figure 3.23: Spectrum of HRV Using Nearest Method.....	46
Figure 3.24: Welch Full Spectrum of HRV Before Downsampling.....	49
Figure 3.25: HRV Signal after Severe Downsampling.....	50
Figure 3.26: Welch Full Spectrum of HRV after Severe Downsampling. ....	52
Figure 3.27: Non-Parametric Spectrum of HRV Signal. ....	53
Figure 3.28: Burg Full Spectrum of HRV Signal. ....	54
Figure 3.29: Parametric Spectrum of HRV Signal. ....	55
Figure 4.1: Histogram of Heart Rate of Relaxed Subject. ....	57
Figure 4.2: Histogram of Peak to Peak Interval of Relaxed Subject. ....	58
Figure 4.3: Histogram of successive Differences of Peak to Peak Interval.....	58
Figure 4.4: Histogram of Heart Rate of Normal Subject.....	60

Figure 4.5: Histogram of Peak to Peak Intervals of Normal Subject.....	60
Figure 4.6: Histogram of successive Differences of Peak to Peak Interval.....	61
Figure 4.7: Histogram of Heart Rate of Stressed Person.....	62
Figure 4.8: Histogram of Peak to Peak Intervals of Stressed Person.....	63
Figure 4.9: Histogram of successive Differences of Peak to Peak Interval.....	63
Figure 5.1: Y-Age Relaxation Patches Packet.....	66
Figure 5.2: Relaxation Patches. ....	66
Figure 5.3: Labelled Explanation of a Patch.....	67
Figure 5.4: Location of Application of a Patch on a Body.....	67
Figure 5.5: Welch Spectrum of Relaxed Subject.....	68
Figure 5.6: AR Spectrum of Relaxed Subject.....	68
Figure 5.7: Welch Spectrum of Normal Subject.....	70
Figure 5.8: AR Spectrum of Normal Subject.....	71
Figure 5.9: Philips Go Lite Therapy.....	73
Figure 5.10: Welch Spectrum before Application of Blue Light.....	74
Figure 5.11: AR Spectrum before Application of Blue Light.....	74
Figure 5.12: Welch Spectrum after Application of Blue Light.....	75
Figure 5.13: AR Spectrum after Application of Blue Light.....	75
Figure 6.1: Block Diagram of Processing of Time Varying Analysis Technique.....	77
Figure 6.2: HRV Signal After Severe Downsampling.....	78
Figure 6.3: Frequency Response of Low Frequency and High Frequency IIR Filters.....	78
Figure 6.4: Low frequency (Blue) and High Frequency (Red) Bands of HRV.....	79
Figure 6.5: Low frequency and High Frequency Power as Function of Time.....	79

Figure 6.6: Ratio of Low Frequency and High Frequency Power as a Function of Time.....	80
Figure 6.7: Standard Spectra Showing Over all Ratio.....	80
Figure 6.8: Severely Downsampled HRV Signal which is a Combination of Relaxed and Stressed State.....	82
Figure 6.9: Variation on Low Frequency and High Frequency Power as a Function of Time.....	83
Figure 6.10: Variation in Low Frequency and High Frequency Ratio as a Function of Time. ....	83

## LIST OF TABLES

Table 3.1: Comparison of Interpolation Results on Non-Parametric Spectrum Estimation.....	47
Table 3.2: Comparison of Interpolation Results on Parametric Spectrum Estimation. ....	48
Table 4.1: Results of Various Time Domain Parameters for Relaxed Subject.....	59
Table 4.2: Results of Various Time Domain Parameters for Normal Subject.....	61
Table 4.3: Results of Various Time Domain Parameters for Stressed Subject. ....	64
Table 5.1: Results of Frequency Domain Analysis Using Patches and FFT Method.....	69
Table 5.2: Results of Frequency Domain Analysis Using Patches and AR Method.....	69
Table 5.3: Frequency Domain Results of Normal Subject Using FFT Method. ....	72
Table 5.4: Frequency Domain Results of Normal Subject Using AR Method.....	72
Table 6.1: Comparison of Time Varying Ratio With FFT and AR Based Ratio.....	81

# **CHAPTER 1**

## **INTRODUCTION**

### **1.1 Objective**

The main objective of this thesis was to design an algorithm that uses biological signal such Photoplethysmogram (PPG) as a source signal to derive the Heart Rate Variability (HRV) signal and perform time- as well as frequency-domain analysis to study the balance of Autonomic Nervous System (ANS) with application to human mental stress estimation.

### **1.2 Background**

#### **1.2.1 Heart Rate Variability (HRV)**

The HRV signal is a measure of variations in beat-to-beat time intervals [1]. It is usually measured in the units of seconds or milliseconds. The time intervals between two beats are usually referred as RR Intervals for an Electrocardiography (ECG) signal and P-P (for peak-to-peak) intervals for a PPG signal. There are numerous methods that could be used for the detection of beats such as ECG, blood pressure, PPG etc. The methods that we chose for beat detection to design the algorithm presented in this thesis were the PPG and the ECG. Analysis of the HRV signal has been widely used as a non-invasive tool for studying the balance of Autonomic Nervous System [1]. Typical HRV analysis techniques include Time-Domain, Frequency-Domain, Geometric, and Non Linear analysis [2]. For this thesis we mainly considered time- and frequency-domain methods for HRV analysis

### 1.2.2 Electrocardiography (ECG)

An ECG signal is primarily used for derivation of HRV [3]. ECG signals are collected using electrodes placed on the body that detect signals that are recorded by a device that is external to the body. Therefore, ECG is a totally noninvasive method to pick up the electrical activity of the heart over a period of time. We used ECG signals to calculate the beat-to-beat time interval and hence derive an HRV signal from it for further analysis and eventually estimating the human mental stress level. All the ECG signals that we use for this research were downloaded from the Physionet website. Figure 1.1 shows a typical ECG signal with beat to beat (R-R) intervals in units of milliseconds (ms).



Figure 1.1: Example of R-R intervals in a ECG Signal [4]

### 1.2.3 Photoplethysmography (PPG)

A PPG signal is recorded using a PPG sensor usually placed on the finger tip. A PPG sensor uses a visible or infrared light emitting diode (LED) and a photodiode to measure blood volume changes in the capillary system with each heartbeat. With each cardiac cycle, the change in blood volume is detected by measuring the amount of light which is transmitted to the photodiode through the tissue [5]. As with the ECG signal, a PPG signal can also be used to detect the beats and thus beat to beat intervals. Figure 1.2 shows an example of a typical PPG signal in comparison with an ECG.

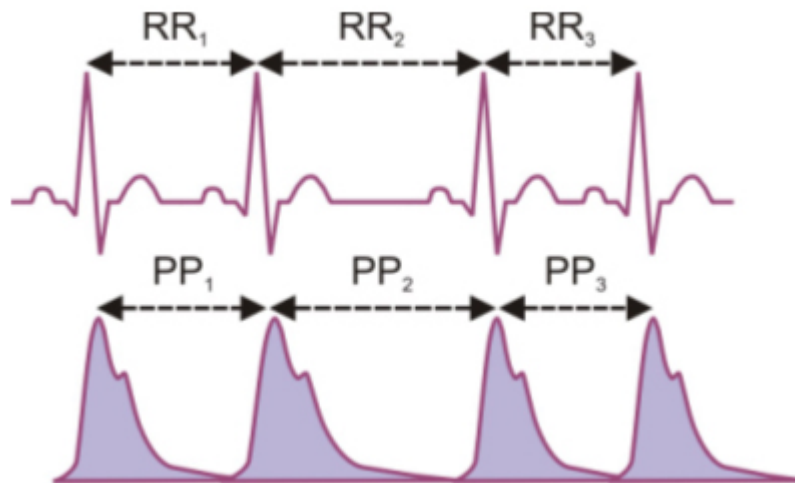


Figure 1.2: Example of P-P intervals in a PPG Signal [6]

The advantage of PPG over ECG is the ease it provides in recording. To record an ECG signal, at least two electrodes have to be placed on the body to detect the electrical activity of the heart [5]. Whereas a PPG sensor can be easily placed on the fingertip and the PPG sensor would also detect the beats through blood pressure activity rather than through electrical activity. We used PPG sensors along with a National Instruments Elvis II board and Matlab's Data Acquisition

Toolbox to record PPG signals and then using them for processing and derivation of HRV for ANS balance estimation.

#### **1.2.4 Autonomic Nervous System**

The ANS is a part of the Nervous System that acts as a control system in the human body [7].

Thus studying the balance of ANS is extremely important in estimating the level of mental stress.

The ANS is divided into two subsystems: Parasympathetic Nervous System and Sympathetic Nervous System. In some cases the two systems act opposite to each other while in some they act together. Figure 1.3 shows how the two ANS subsystems affect the different body parts:

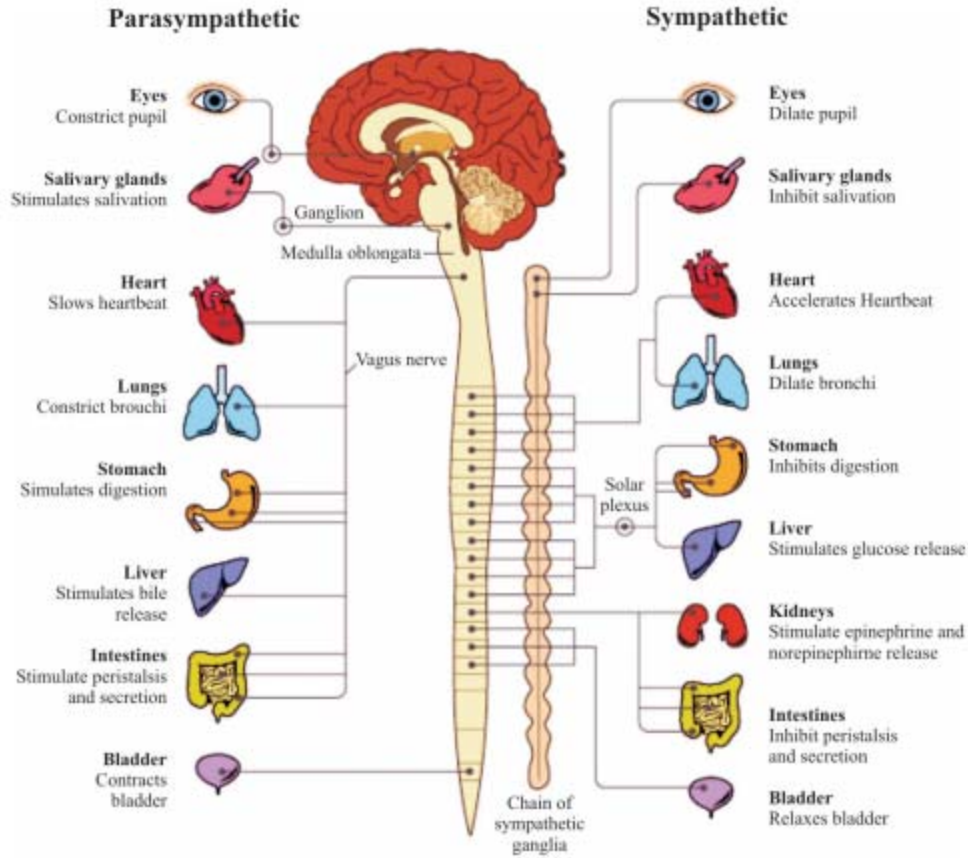


Figure 1.3: Example of Autonomic Nervous System Regulating Functioning of organs [8]

Spectral analysis of Heart Rate Variability (HRV) has been widely used as a noninvasive tool for studying the state of the ANS [1]. The HRV signal contains the frequency components associated with the sympathetic and parasympathetic part of the Autonomic Nervous System [2] thus; a successful separation of these components in the HRV Spectrum can be used to assess the human mental stress. HRV spectrum is divided into Very low Frequency band (0-0.04 Hz), Low Frequency band (0.04-0.15 Hz), High Frequency band (0.15-0.4 Hz) and Very High Frequency band ( $\geq 0.4$  Hz) [2] where more High Frequency components represent vagal dominance whereas more Low Frequency components represent stress. Therefore, the Low Frequency to High Frequency ratio index could be used as a noninvasive marker of mental stress level.

### **1.2.5 Time Domain Analysis**

Once an HRV signal is derived using an ECG or a PPG signal there are a number of methods that could be employed for analysis. The most common analysis method is Time Domain Analysis. Usually, it is performed on two kinds of data.

- a) Analysis done directly on the measurement of Peak-to-Peak (P-P) intervals.
- b) Analysis done on the successive differences between pairs of P-P intervals [2].

The various time domain measurement techniques that are used for the analysis of HRV are;

- Standard Deviation of P-P intervals (SDP-P)
- Standard Deviation of Average P-P Intervals (SDAP-P)
- Root mean square of successive P-P differences (RMSSD)
- Standard Deviation of differences between adjacent P-P intervals (SDSD)
- Histogram of Successive Differences
- Histogram of P-P intervals.
- Histogram of (instantaneous) Heart Rate values.
- Number of pairs of adjacent P-P intervals differing by more than 50 ms in the entire recording (NN50)
- NN50 count divided by the total number of P-P intervals (pNN50) gives as a percentage

A detailed result of this analysis is shown in chapter 3.

### **1.2.6 Frequency Domain Analysis**

Frequency domain analysis typically requires interpolating the P-P intervals to produce a continuous HRV signal as a function of time. Next, the interpolated HRV signal is decimated to lower rates, typically 2 Hz or 4 Hz (2 or 4 samples/second) [1]. Once the HRV signal at a reduced rate is produced, spectral analysis is performed to generate an HRV spectrum which is then divided into low frequency or LF (0.04-0.15Hz) and high frequency or HF (0.15-0.4Hz) regions to compute the total power under these regions to estimate the dominance of sympathetic or parasympathetic part of the ANS. Usually, ANS balance is estimated by computing the LF/HF ratio of signal power in the two regions; higher ratio suggests more Sympathetic Nervous System dominance and lower ratio suggests more Parasympathetic dominance. For spectral analysis we used parametric and non-parametric methods [2]. Figure 1.4 is an example of spectral estimation results and the resulting ratio.

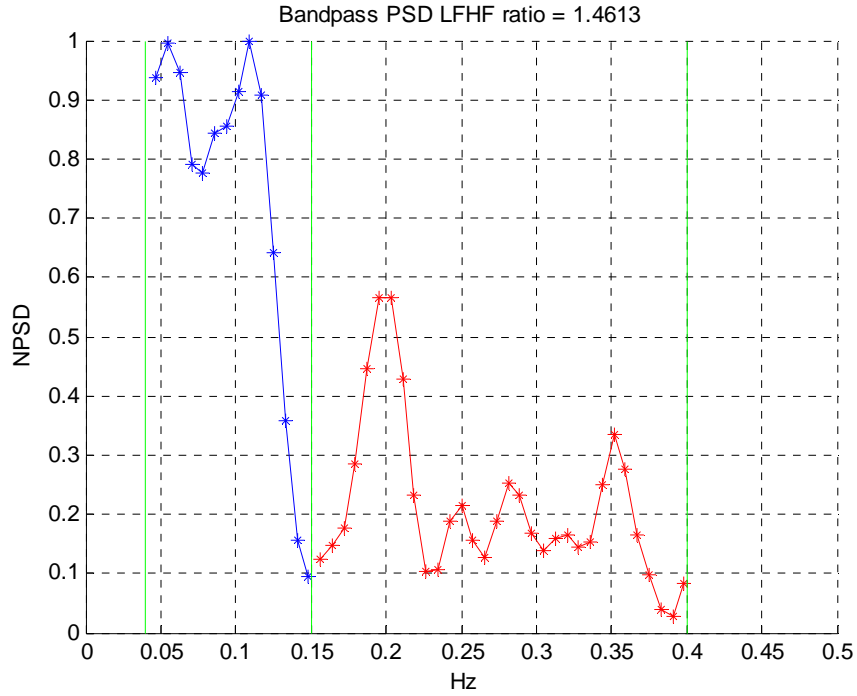


Figure 1.4: Power Spectral Density of a HRV Signal

### 1.3 Motivation

The main motivation behind this research was to develop an algorithm that takes an input PPG signal and performs various processing steps to eventually produce a mental stress index. The details are given in figure 1.5 which represents an overall block diagram with a step-by-step working of the algorithm that we designed. Another motivation, also shown in figure 1.5, was to choose subjects and test conditions that could produce different mental stress index values.

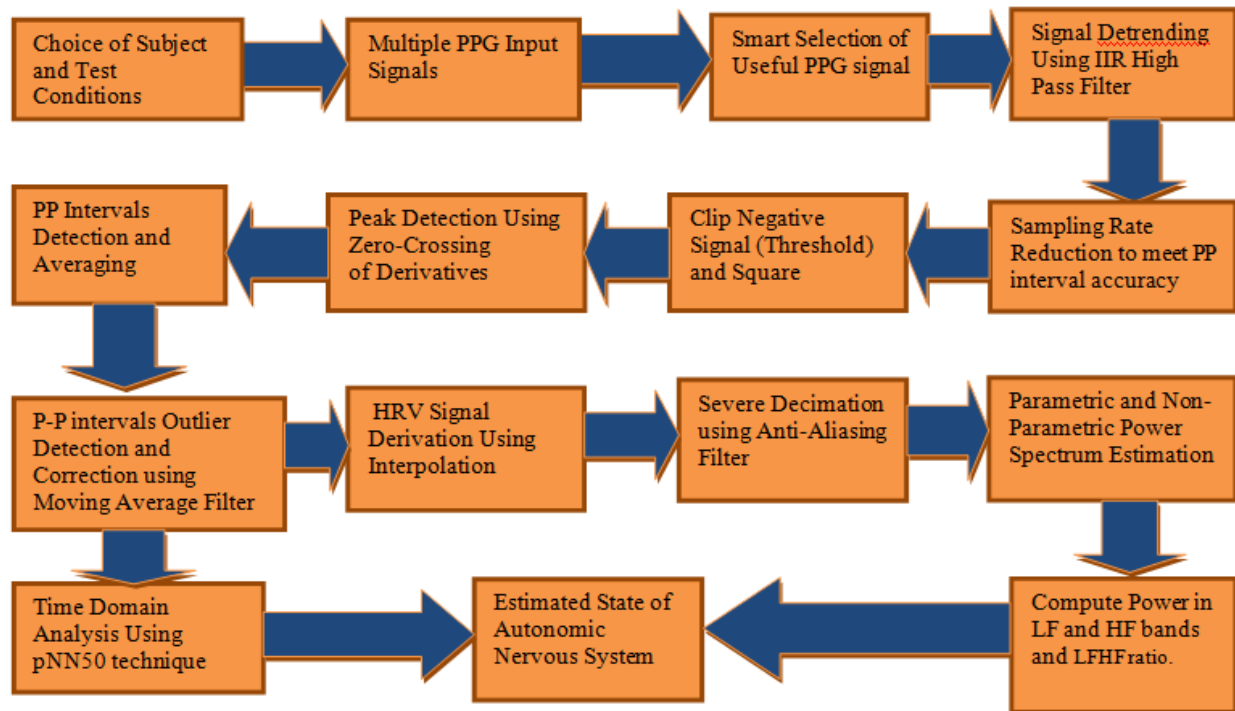


Figure 1.5: Overall Block Diagram of all the processing done to arrive at a Mental Stress Index.

## **CHAPTER 2**

### **LITERATURE REVIEW**

#### **2.1 Heart Rate Variability**

Heart Rate Variability (HRV) is a measure of variation in beat-to-beat interval (N-N) over a period of time. It has been widely used as a noninvasive marker for studying the balance of Autonomic Nervous System and it is relatively easy to derive [1]. It is one of the various measure obtained from the biological signals that provide significant knowledge about the balance of the ANS.

The significance of HRV dates back to 1965 when Hon and Lee found that fetal distress resulted in alterations in inter-beat intervals. During the 1970s, Ewing et al, devised a number of simple bedside tests of short term N-N differences to detect autonomic neuropathy in diabetic patients. In 1977, Wolf et al first showed the association of higher risk of post infarction mortality with reduced HRV signal variance. Introduction of Power Spectral analysis of heart rate fluctuation for quantitatively evaluating beat-to-beat cardiovascular control was done by Akselrod et al in 1981. In late 1980, the importance of HRV became apparent with confirmation of HRV as a strong and independent predictor of mortality following an acute myocardial infarction. Today with the availability of new digital high frequency, multiple channel signal recorders, HRV has gained potential as a provider of additional valuable insight about physiological and pathological conditions [2].

## 2.2 HRV Derivation

Heart Rate Variability signal is typically derived from an Electrocardiograph (ECG). ECG is a graphical recording of electrical activity of the human heart [1, 9]. This electrical activity is the result of the depolarization and repolarization of atria and ventricles. Depolarization is said to occur when electrically polarized cardiac cells lose their internal negativity. As depolarization travels from cell to cell a depolarization wave is produced across the entire heart. This wave represents a flow of electricity and gets detected by electrodes placed on body surfaces. Once the depolarization is complete, the cardiac cells get restored to their resting potential and this process is known as repolarization. This occurrence of polarization and repolarization gives rise to a ECG waveform which consist of P wave, QRS complex, T wave and finally U wave per cardiac cycle [9]. Figure 2.1 shows a typical electrocardiogram (ECG)

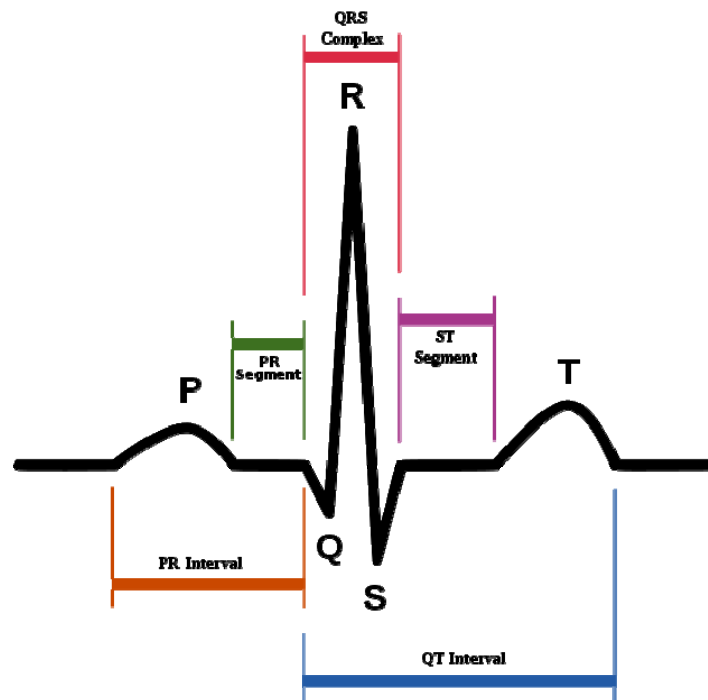


Figure 2.1: A Typical Electrocardiogram Signal [10]

ECG recording can be a complex process as it requires that at least two electrodes to be connected to human body. Each heartbeat is a result of section of heart producing electrical activity which is recorded from the skin using appropriate electrodes. To record an ECG, 2, 3, 6, 10, 12 or 16 electrodes can be fixed to the body of the subject [11].

Other than ECG, the HRV can also be derived using a PPG signal. The multiple-electrode drawback can be overcome by using a photoplethysmographic (PPG) signal for deriving the HRV. A PPG sensor uses a combination of an LED and a photodiode to measure a blood volume change in the capillary system. During each cardiac cycle, the blood volume change is detected by quantifying the amount of light that is transmitted to a photodiode through tissue [5].

A human heart is divided into four chambers: left and right ventricles and left and right atrias. The right ventricle pumps the blood to the lungs where blood gets oxygenated. The oxygenated blood then enters the left atrium then the blood passes to the left ventricles through a valve which then pumps the blood to the rest of the body. The deoxygenated blood reaches the right atrium. The contraction of ventricles is called systole and the relaxation of ventricles is called diastole. During diastole the ventricles are refilling. Thus, the period of PPG is split into two parts the rising phase which is called systolic time and the falling phase which represent diastolic time [11].

### **2.3 Autonomic Nervous System**

Autonomic Nervous System is a part of the Nervous System and acts as a system that controls the cardiac muscle. Thus studying the balance of ANS is extremely important in estimating the

level of mental stress. ANS affects heart rate, digestion, respiratory rate, perspiration, pupillary dilation, salivation etc. ANS is divided into two subsystems Parasympathetic Nervous System and Sympathetic Nervous System. In some cases the two systems acts opposite to each other while in some they act together [12]. ANS activity, which comprises of the activities of the sympathetic and parasympathetic together, influence the sinus node of the heart therefore modulating heart rate. The sympathetic activity is primarily responsible for preparing body for stress related situations by boosting energy. On the contrary the parasympathetic activity tries to overcome the effects of sympathetic activity and restores the body to a resting state. Parasympathetic activity is most active during a restful state. Under normal conditions the two activities show a balance between them however, during rest this balance changes and sympathetic activity starts dominating [13].

As mentioned earlier, the HRV signal contains frequency components that could be divided into ultra-low frequency (0.0001-0.003 Hz), very low frequency components (0.003-0.04 Hz), low frequency components (0.04-0.15 Hz) and high frequency components (0.15-0.4 Hz) [2]. Traditionally it is believed that high frequency is affected by parasympathetic activity whereas low frequency is affected by sympathetic activity. Thus the ratio of power associated with low frequency region and high frequency region is used to study the balance of Autonomic Nervous System. The very low frequency component is associated with factors like hormone, temperature etc. [13]

## **2.4 HRV Analysis**

Analysis of HRV is typically categorized into time- and frequency-domain analysis. With time domain analysis techniques parameters such as mean heart rate, distance between longest and shortest NN interval, difference between night and day time heart rate, etc. can be calculated. Statistical analysis is usually divided into two parts: a) those derived from the direct measurements of the NN intervals or instantaneous heart rate; b) those derived from the differences between the NN intervals. These variables can be derived by analyzing the whole recording of the signal or by dividing the whole signal into multiple segments. The later method is preferred as it allows result to be compared between different segments such as comparison of day time vs. night time recording results, sleep vs. wakefulness recording results, etc. [2]

The overall variables that are calculated under time domain analysis techniques are listed in figure 2.2 [2].

Variable	Units	Description
Statistical measures		
SDNN	ms	Standard deviation of all NN intervals.
SDANN	ms	Standard deviation of the averages of NN intervals in all 5 min segments of the entire recording.
RMSSD	ms	The square root of the mean of the sum of the squares of differences between adjacent NN intervals.
SDNN index	ms	Mean of the standard deviations of all NN intervals for all 5 min segments of the entire recording.
SDSD	ms	Standard deviation of differences between adjacent NN intervals.
NN50 count		Number of pairs of adjacent NN intervals differing by more than 50 ms in the entire recording. Three variants are possible counting all such NN intervals pairs or only pairs in which the first or the second interval is longer.
pNN50	%	NN50 count divided by the total number of all NN intervals.

Figure 2.2: Various Time Domain Parameters in HRV Analysis (table taken from [2]).

Other authors have used 14 different variables to determine and index subjects, dividing them into low and high stress groups [14].

Frequency domain analysis is also used for estimating the balance of the Autonomic Nervous System. In frequency domain analysis the non-parametric and parametric Power Spectral Density (PSD) of the HRV signal is calculated. The PSD is split into very low frequency, Low Frequency (LF) (0.04-0.15Hz) and High Frequency (HF) (0.15-0.4 Hz) regions. The total power in the respective region is calculated and their ratio (LF/HF) is calculated to estimate the balance of the sympathetic and parasympathetic activity. The non-parametric is a Fast Fourier Transform (FFT)

based approach whereas the parametric method is an Auto Regressive (AR) based approach to estimate the PSD of the HRV signal [2].

PSD analysis provides information about how the power has been distributed as a function of frequency. Literature review indicates that both the non-parametric and parametric method provides comparable results. However, there are some advantages of non-parametric method over parametric method. These advantages are [2]:

- a) Simplicity of the algorithm employed as they are based on FFT computations.
- b) Fast processing speed.

Some advantages of parametric method are [2]:

- a) Smoother spectral components.
- b) Easy post processing of the spectrum and easy identification of central frequency of each spectrum.
- c) Accurate estimation of PSD even on small number of samples over which the signal is supposed to maintain stationarity.

The basic disadvantage of parametric PSD estimation is the verification of the model chosen i.e. the order of the model and complexities associated with it [2].

Short term recording are those which have a recording length between 2 and 5 minutes. Whereas long term recordings have a recording length of 24 Hrs. The spectral components are divided into Ultra Low Frequency (ULF), Very Low frequency (VLF), Low Frequency (LF) and High Frequency (HF). Figure 2.3 shows the distribution of various frequency components in the PSD of the HRV signal [2].

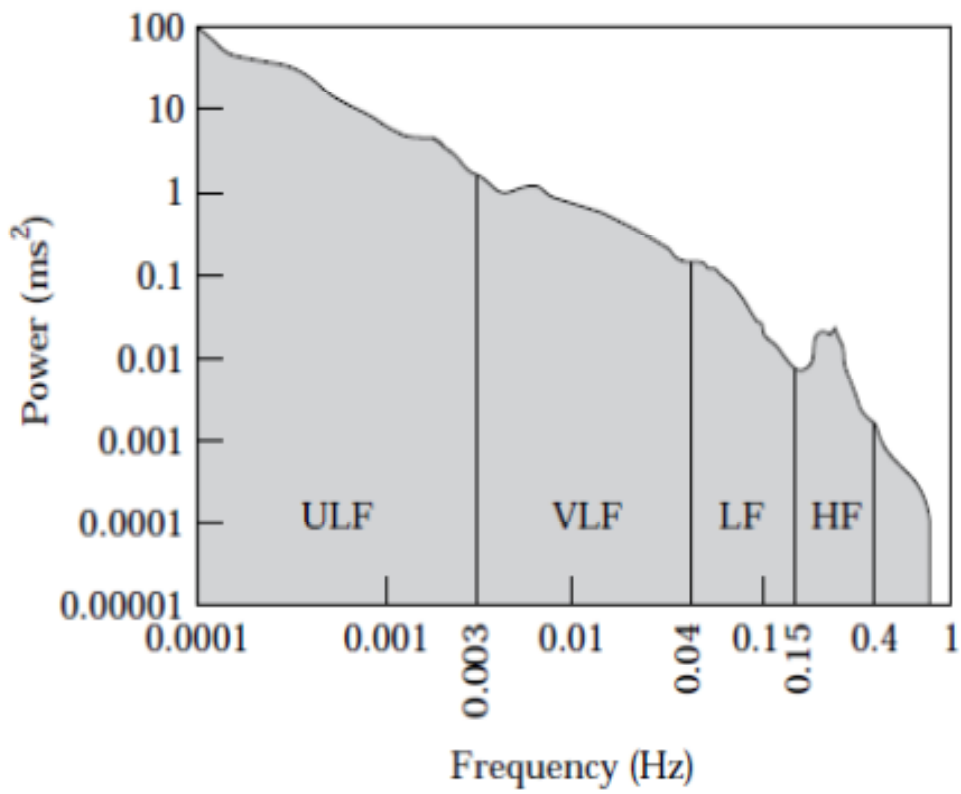


Figure 2.3: Spectral Regions of Typical Power Spectral Density [2]

Also, figure 2.4 shows various spectral components considered in short term vs. long term recording.

Variable	Units	Description Analysis of short-term recordings (5 min)	Frequency range
5 min total power	ms <sup>2</sup>	The variance of NN intervals over the temporal segment	approximately $\leq 0.4$ Hz
VLF	ms <sup>2</sup>	Power in very low frequency range	$\leq 0.04$ Hz
LF	ms <sup>2</sup>	Power in low frequency range	0.04–0.15 Hz
LF norm	n.u.	LF power in normalised units $LF / (Total\ Power - VLF) \times 100$	
HF	ms <sup>2</sup>	Power in high frequency range	0.15–0.4 Hz
HF norm	n.u.	HF power in normalised units $HF / (Total\ Power - VLF) \times 100$	
LF/HF		Ratio LF [ms <sup>2</sup> ]/HF [ms <sup>2</sup> ]	
Analysis of entire 24 h			
Total power	ms <sup>2</sup>	Variance of all NN intervals	approximately $\leq 0.4$ Hz
ULF	ms <sup>2</sup>	Power in the ultra low frequency range	$\leq 0.003$ Hz
VLF	ms <sup>2</sup>	Power in the very low frequency range	0.003–0.04 Hz
LF	ms <sup>2</sup>	Power in the low frequency range	0.04–0.15 Hz
HF	ms <sup>2</sup>	Power in the high frequency range	0.15–0.4 Hz
$\alpha$		Slope of the linear interpolation of the spectrum in a log-log scale	approximately $\leq 0.04$ Hz

Figure 2.4: Various Frequency Domain Parameters (Long Term Vs. Short Term) [2]

## 2.5 Data Collection

Electrocardiogram signals for research and verification of algorithm can be obtained from MIT-BIH Arrhythmia Database [15]. The MIT-BIH Arrhythmia Database contains two channel ECG recordings which were acquired from 47 subjects who were studied by the BIH laboratory between 1975 and 1979. Twenty three recordings were chosen from 4000 ECG recordings acquired from mixed populations of inpatients (60%) and outpatients (40%) at BIH. The other 25% were selected from the same set to include less common but clinically significant arrhythmias. The signals were sampled at a sampling rate of 360 samples per second with 11 bit resolution over a 10 mV range [15]. All these data can be freely accessed by installing a WFDB

Software package for Matlab [15]. Previously authors have used data from this source to verify their research [9]. A pertinent literature review indicates that it is important to sample the signal at relatively high rates (usually over 300 Hz) to accurately detect the peaks [16, 17]. Sampling the signal at much low rates produces jitters and thus could lead to inaccurate detection of peaks and finally false estimation of mental state. Literature review also indicates that lower sampling rate ( $\geq 100$  Hz) may also work satisfactorily only if proper interpolation is used to refine the R wave fiducial point [2].

## **2.6 Peak Detection and HRV Derivation**

Previously, researchers have proposed many techniques for detecting peaks from ECG and PPG signals. Such of these techniques include: wavelet transform, differentiation, Hilbert transform, enhanced Hilbert transform, digital filters, etc. [1, 9]. A thresholding step has also been discussed in the literature to further refine the accuracy of the detection of peaks for NN interval detection. Usually adaptive thresholding is considered better than fixed thresholding since fixed thresholding doesn't work well with amplitude varying signals and tends to result in missing peaks [18]. Manual checking for detection of any missed peak is also a common practice and some algorithms have been proposed to declare when a peak has been missed and a measure to correct it. Although it is also mentioned that manual editing should be minimized as time and frequency domain analysis of such signal tends to produce biased result [2], [18]. After detecting accurate peaks, the distance between the peaks (N-N interval) are calculated in the units of seconds. These NN intervals are also termed as a discrete event series (DES). A non-uniform interpolation scheme is then performed to obtain a continuous Heart Rate Variability signal as a function of time. Both parametric and non-parametric methods could be applied for the analysis

of the continuous HRV signal (obtained after interpolating the DES). However, it is recommended in literature that the parametric method be used [2]. Figure 2.5 shows typical processing steps recommended by the Task Force of The European Society of Cardiology and The North American Society of Pacing and Electrophysiology [2]

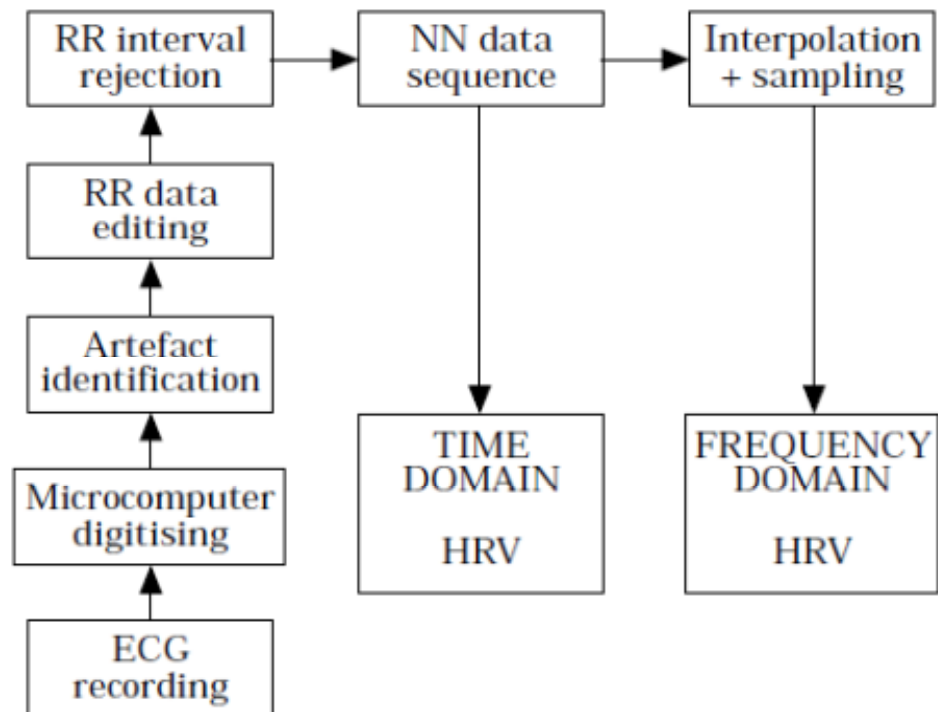


Figure 2.5: Typical Signal Processing Steps [2]

## 2.7 Correlation between Time and Frequency Domain Analysis

Both time- and frequency-domain methods have been used in the literature for HRV analysis. Although frequency domain methods are clearer marker of the balance of Autonomic Nervous system, there have been researchers who used solely time-domain parameters to differentiate between stress and non-stress states. The possibility of using time-domain parameters as an alternative to the LF/HF ratio has been explored [19, 20]. Thus understanding correlation between time and frequency domain parameters becomes an interesting study. Figure 2.6 shows existing significant correlations between time and frequency domain measures found in the literature [2]

Time domain variable	Approximate frequency domain correlate
SDNN	Total power
HRV triangular index	Total power
TINN	Total power
SDANN	ULF
SDNN index	Mean of 5 min total power
RMSSD	HF
SDSD	HF
NN50 count	HF
pNN50	HF
Differential index	HF
Logarithmic index	HF

Figure: 2.6 Typical Correlations between Time and Frequency Domain Analysis [2]

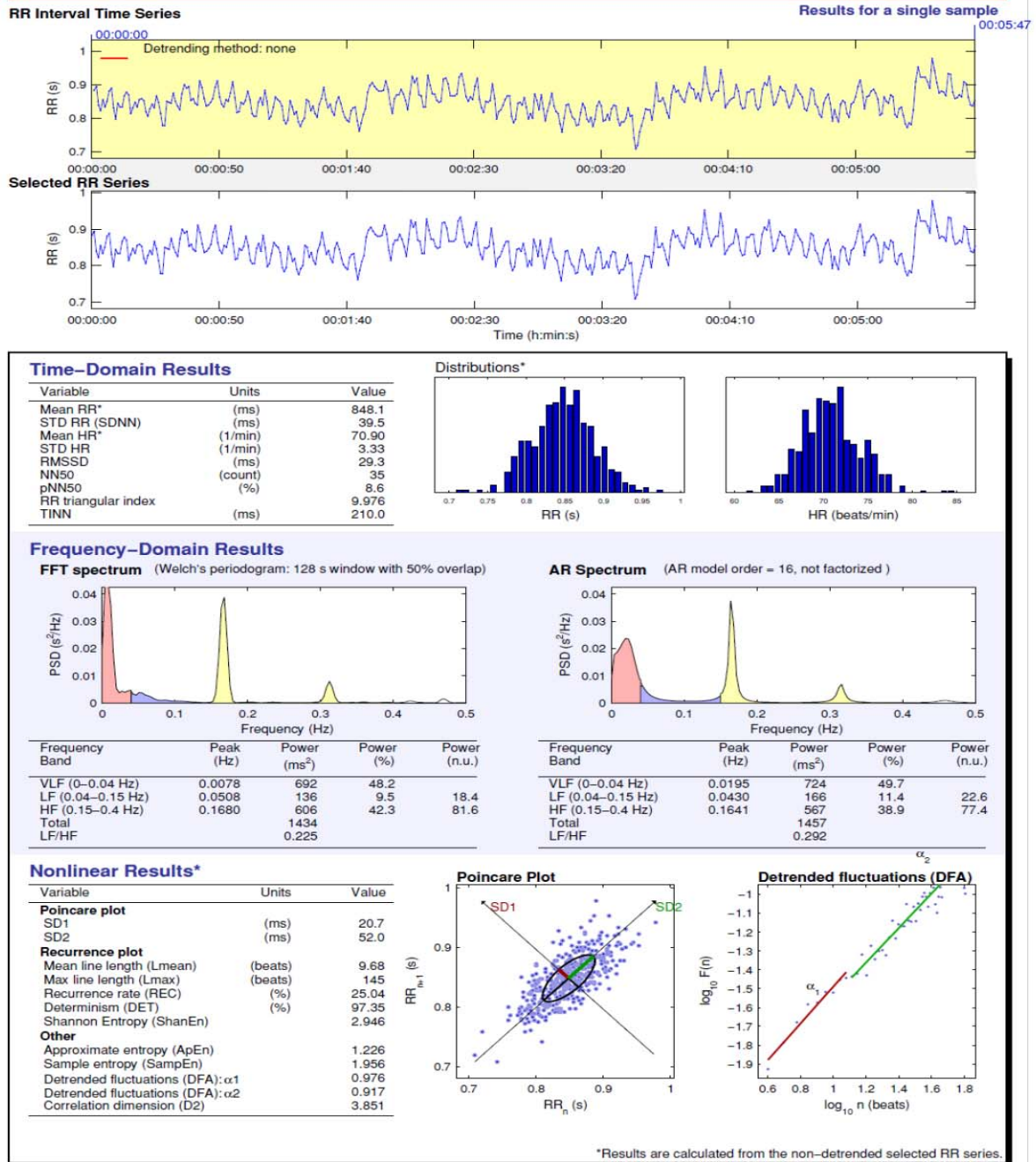
## **2.8 Existing HRV Analysis Software**

Kubios is HRV analysis software that interpolates a DES signal, performs time-domain, frequency-domain and nonlinear analysis. The user feeds an N-N signal and the software produces all the analysis results, and the user can also save a pdf file as a report. This software can be downloaded for free from Internet [21]. There have been other software packages that have been developed or are in development [22]. Figure 2.7 is example report generated by the Kubios HRV analysis software [21]. This Software uses a detrending scheme as mentioned in [23] .

# HRV Analysis Results

RR\_Final.txt - xx/xx/xx - xx:xx:xx

Page 1/1



20-Sep-2013 09:04:45

Ajay Verma

Electrical and Computer Engineering, The University of Texas at El Paso (UTEP)

Kubios HRV, version 2.0

Department of Physics

University of Kuopio, Finland

Figure 2.7: KUBIOS HRV Analysis Report

## **2.9 Accuracy of PSD Based Estimation**

As mentioned before the LF/HF index has been used as a marker of balance of ANS. For example high ratio indicates sympathetic dominance whereas low ratio indicates parasympathetic dominance. It is also believed that low frequency is affected by both sympathetic and parasympathetic activity and high frequency is solely affected by parasympathetic activity. Thus, LF/HF index is an imperfect approximation of the balance of the autonomic nervous system. The literature also reveals that physiological mechanisms that are responsible for heart rate fluctuations have nonlinear components and since the LF/HF index is based on linear processing, it does not consider the nonlinear characteristics of the ANS. Therefore, a new method is required that takes into account the nonlinear components responsible for heart rate fluctuations. [16] [17].

## **2.10 Principle Dynamic Mode (PDMs)**

The method of Principal Dynamic Modes (PDMs) decomposition seem to address the above mentioned problem and it can separate the nonlinear dynamics of the Autonomic Nervous System [16, 17]. The nonlinear PDM method was first introduced by Marmarelis and was applied to the analysis of physiological systems. The PDMs are calculated using Volterra-Weiner kernels based on the expansion of Laguerre polynomials [24]. Some work has been done already using this technique to quantify the state of the autonomic nervous system and the authors found that the PDM method produces slightly better results than PSD method [25], [26].

### **2.11 Effects of Light on ANS**

Blue enriched light has been used to enhance the mood of people. The blue light therapy claims to provide promising results to treat subjects suffering from Seasonal Affect Disorder (SAD) [27-29].

## **CHAPTER 3**

### **ALGORITHM FEATURES**

#### **3.1 Data Collection**

All the ECG data that were used in this research were collected from the Physionet website [15] using WFDB toolbox. All the physionet's ECG data were sampled at 360 Hz. The entire PPG signals that we used were recorded in our own biomedical engineering laboratory using one or three PPG sensors (Easy Pulse kit: A DIY pulse sensor based on photoplethysmography from tindie.com), a National Instruments Elvis II board, and Matlab's Data Acquisition Toolbox. The PPG signals were mostly recorded at 1000 samples/second for maximum flexibility.

##### **3.1.1 A Multiple Sensor Concept**

As part of the research documented in this thesis, we briefly explored the idea of using multiple sensors to record PPG signals. Sensors were put on more than one fingers of a person to collect signals from different fingers. Using multiple signals one signal was created as a combination of the entire signal available using a simple coherent averaging technique. This allowed us to get rid of any loss in contact occurred with sensor while recording signals. The simplicity of the approach is possible due to the adaptive nature of the signal processing done to find the peaks in the PPG signal. Figures below shows three different PPG signals (after detrending with a high-pass filter) collected from different fingers and the resulting averaged signal. The recorded signals suffered loss of contact at different time interval and then we showed that the averaging technique can be used to overcome this problem.

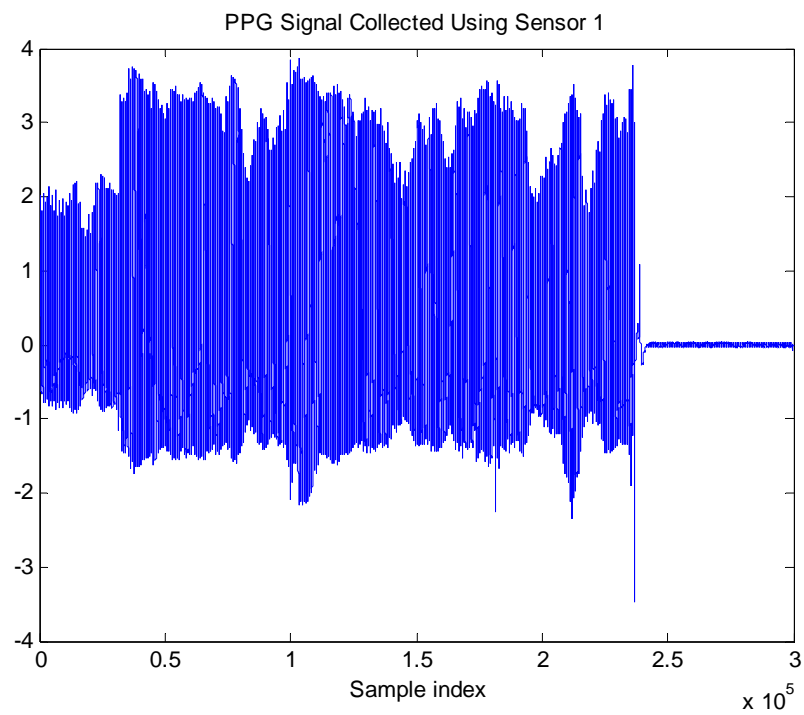


Figure 3.1: A PPG Signal Collected Using Sensor 1 after detrending.

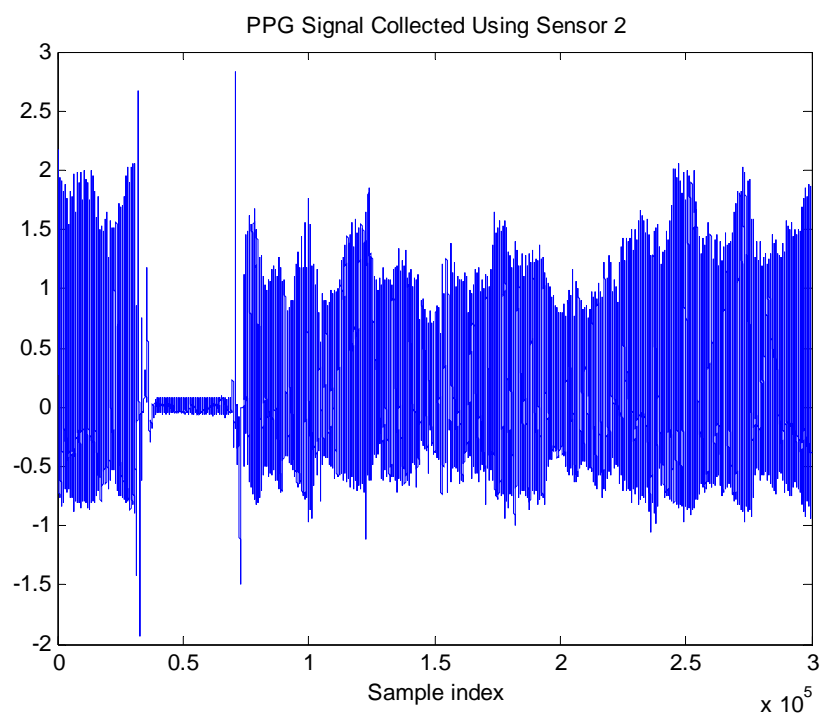


Figure 3.2: A PPG Signal Collected Using Sensor 2 after detrending.

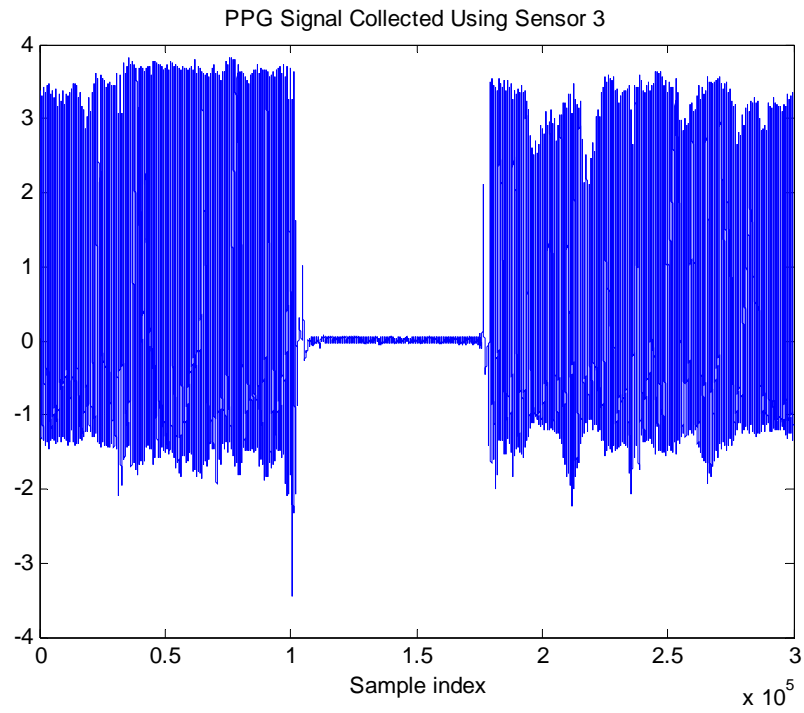


Figure 3.3: A PPG Signal Collected Using Sensor 3 after detrending

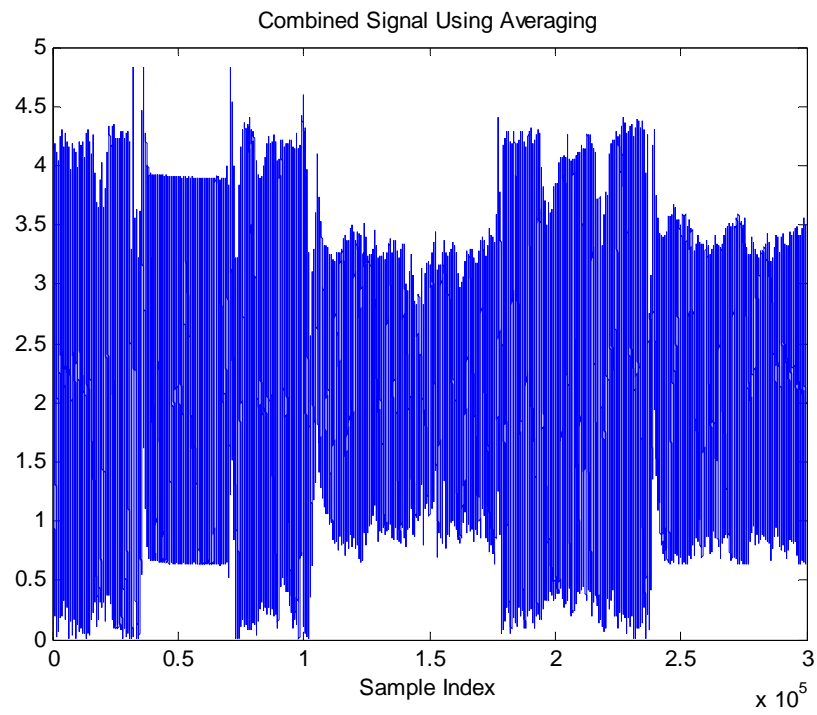


Figure 3.4: Combined PPG Signal Using Coherent Averaging technique

### 3.2 Sampling Rate Reduction

Since the original PPG signals were sampled at a very high rate of 1000 Samples/Second (SS), and since the bandwidth of the signals was found to be well below 40 Hz, the original signal can be decimated down to a rate of 80 SS without needing an anti-aliasing filter. According to the Nyquist sampling theorem, we should sample at twice the bandwidth (BW) of a low-pass band limited signal:

$$F_s > 2(BW)$$

Sampling rate reduction speeds up the processing time without causing aliasing if the signal has been decimated to a lower rate approaching the minimal (Nyquist) rate. Figure 3.5 shows the spectrum of the original signal using a decibel vertical scale clearly showing the essential bandwidth of 40 Hz. Beyond that frequency, the spectrum is more than 50 dB below its maximum value.

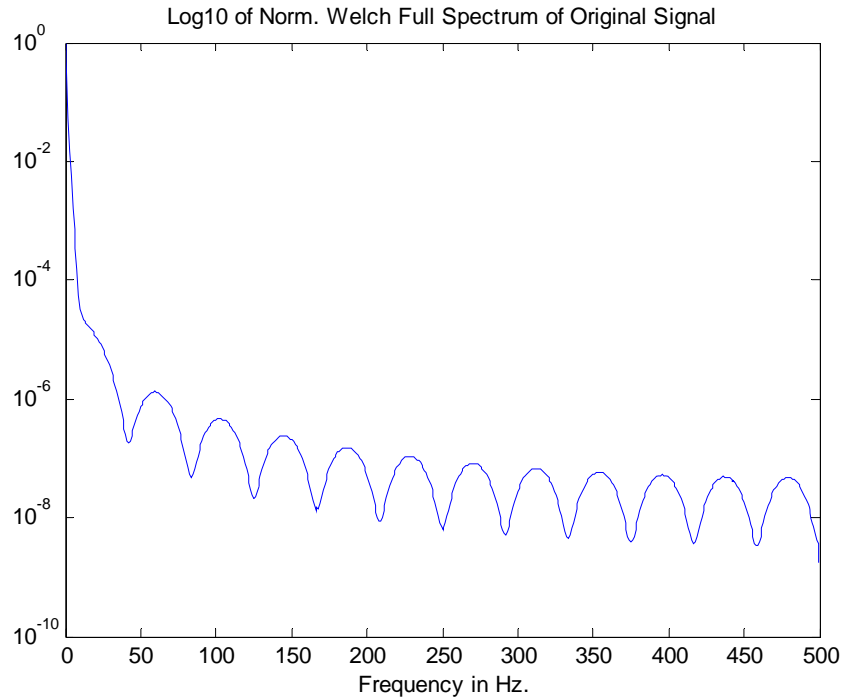


Figure 3.5: Full Spectrum of Original Signal Sampled at 1000 Hz

This degree of severe oversampling allowed us to consistently reduce the sampling rate and process the signals at lower rates to speed up the processing time. The Welch spectra that we obtained by processing the signals at different rates were very similar at low frequencies. Figure 3.6 and 3.7 show the HRV spectra of a signal processed mostly at 1000 SS and the same signal processed mostly at 100 SS.

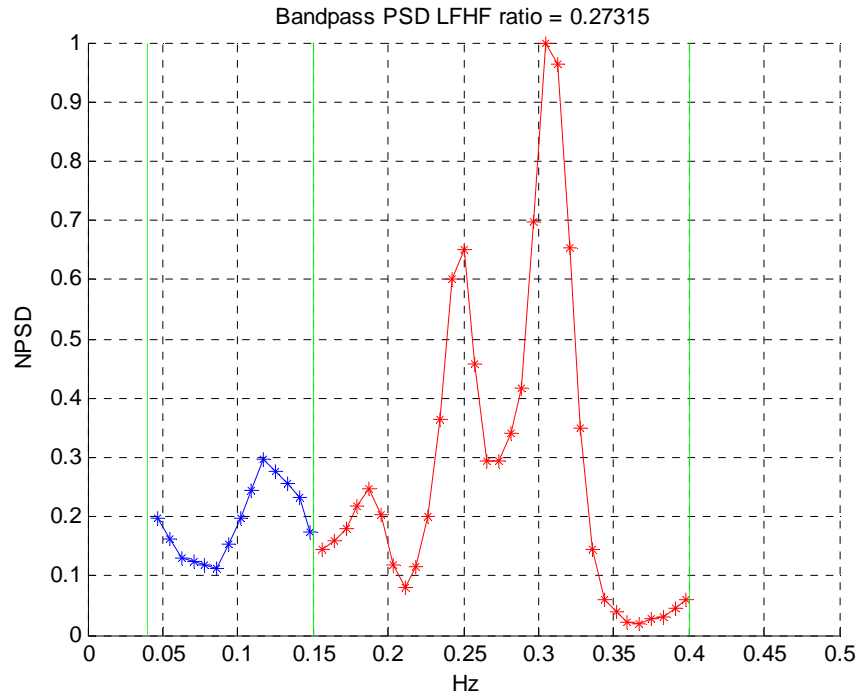


Figure 3.6: HRV PSD Derived from a Signal Processed Mostly at 1000 Samples/Sec.

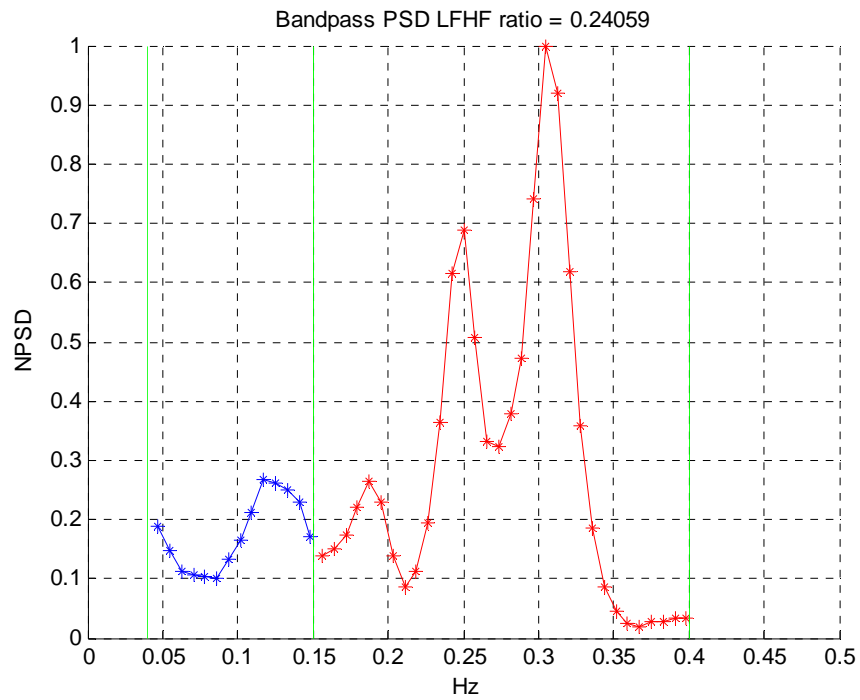


Figure 3.7: HRV PSD Derived from a Signal Processed Mostly at 100 Samples/Sec.

### 3.3 Preprocessing

Usually the raw ECG/PPG signals have high and low frequency noises that get incorporated into while recording. Most sensors would have automatic high-frequency noise rejection of while most would not reject low-frequency noise (unwanted trends). Therefore, it is always better to preprocess the signals to get rid of low frequency trends. The two preprocessing filters that were considered for our algorithm were a simple Infinite Impulse Response (IIR) high-pass filter and a 1-d Discrete Wavelet Transform Daubechies-6 Finite Impulse Response (FIR) filter. The IIR filter proved to be sufficient and the other approach was not considered further. The use of the discrete wavelet transform, which provides time-frequency representation of the signal and is very well suited for non-stationary signals like ECG or PPG was considered for more general analysis though it is not mentioned further in this thesis. A typical block diagram of preprocessing step based on IIR filters is shown in figure 3.8.



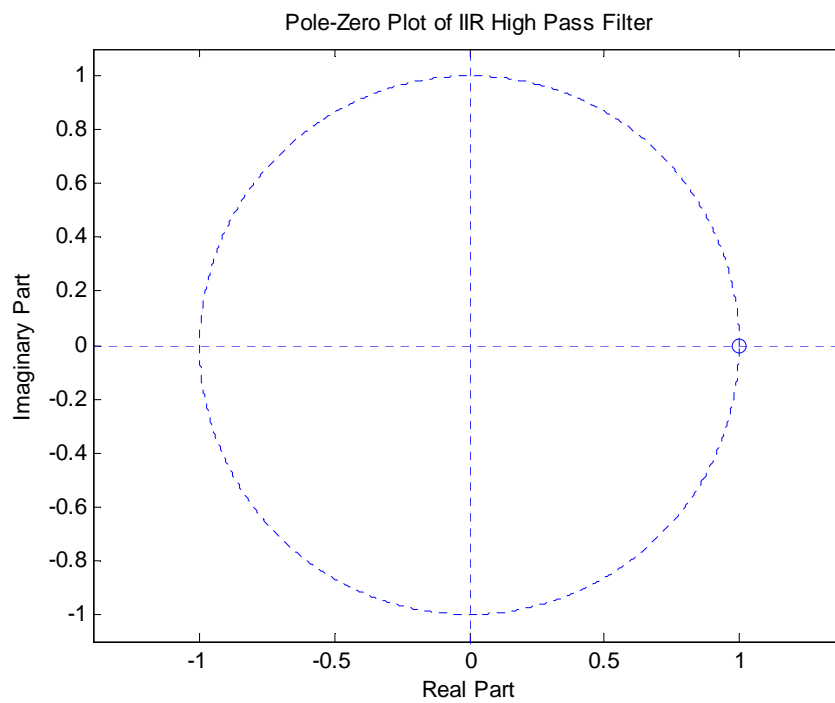
Figure 3.8: Preprocessing Steps to Detrend the PPG Signal.

We used a simple IIR high-pass filter with the following transfer function for removing trends from the input signal

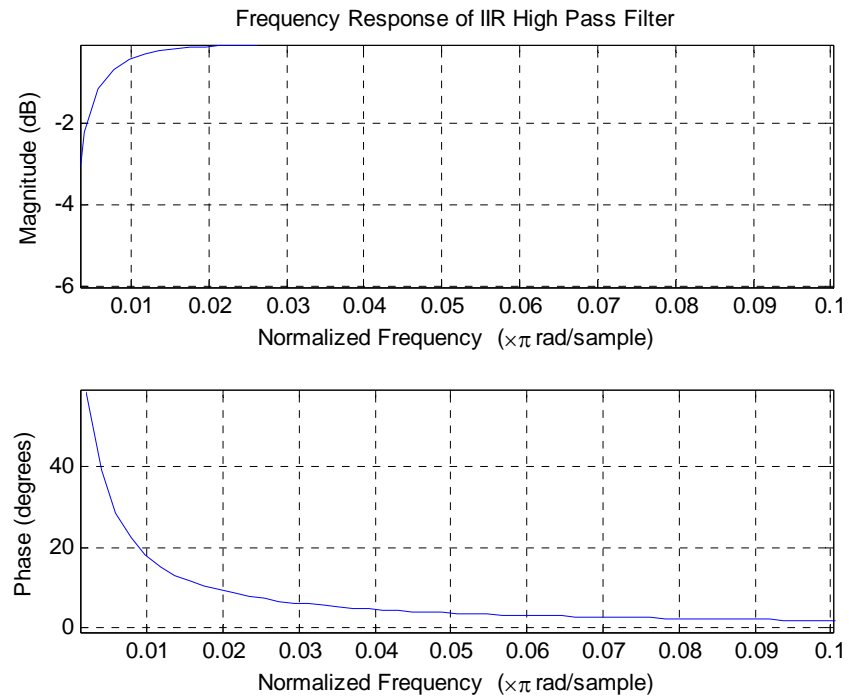
$$H(z) = \frac{1+\alpha}{2} \frac{1-z^{-1}}{1-\alpha z^{-1}}$$

Where the value of  $\alpha$  used to produce a very narrow notch was chosen to be 0.99.

Figure 3.9 a) and b) shows the pole-zero plot and a frequency response plot of this IIR filter. Clearly, the phase of the filter is nearly linear at very low frequencies, a desirable property since peak locations would not be affected. Figures 3.10 and 3.11 shows an original and a preprocessed signal respectively:



a)



b)

Figure 3.9: Pole-Zero a) and Frequency Response of IIR High Pass Filter

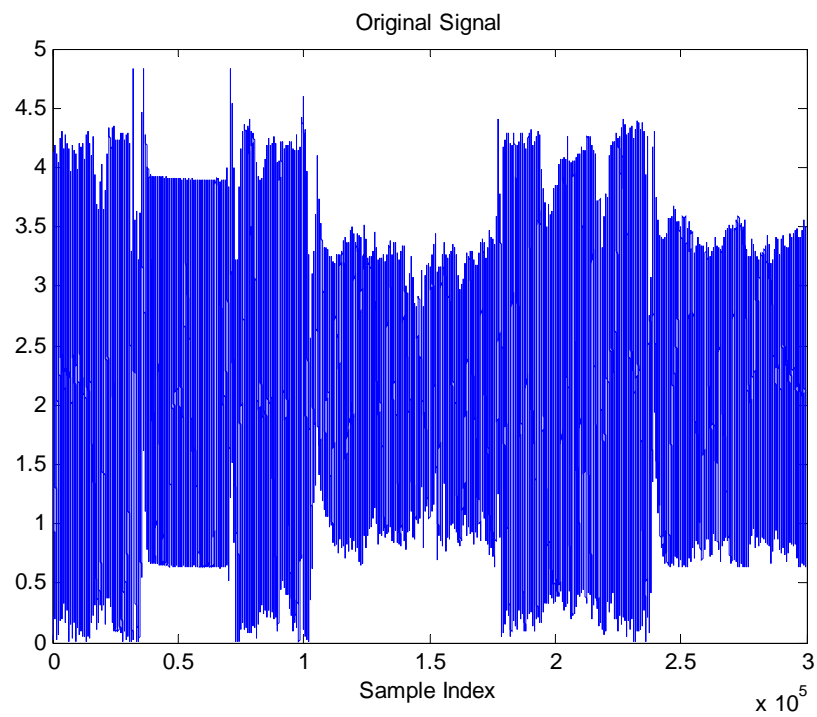


Figure 3.10: Original Signal

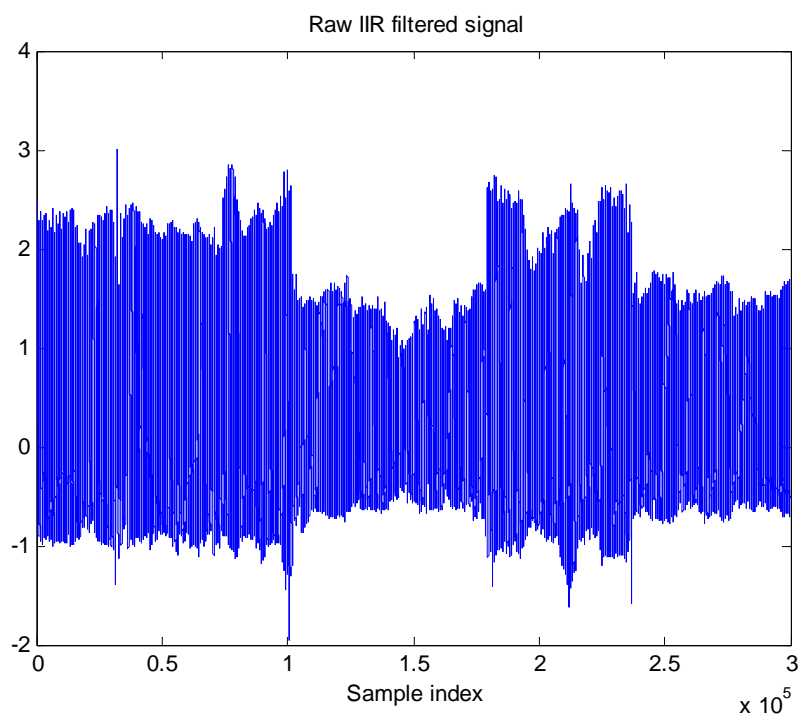


Figure 3.11: Pre-Processed Signal using IIR High Pass Filter

### 3.4 Thresholding and Peak Detection

Once the preprocessed signal is obtained, the next step is to discard the non-positive peaks as the negative peaks can never be candidates for PPG signal peaks associated with heart beats . This step is followed by squaring the positive peaks to increase the dynamic range of the beats (actual peak) compared to rest of the peaks which are not candidates for actual beat peak. Figure 3.12 is an example of one such processing:

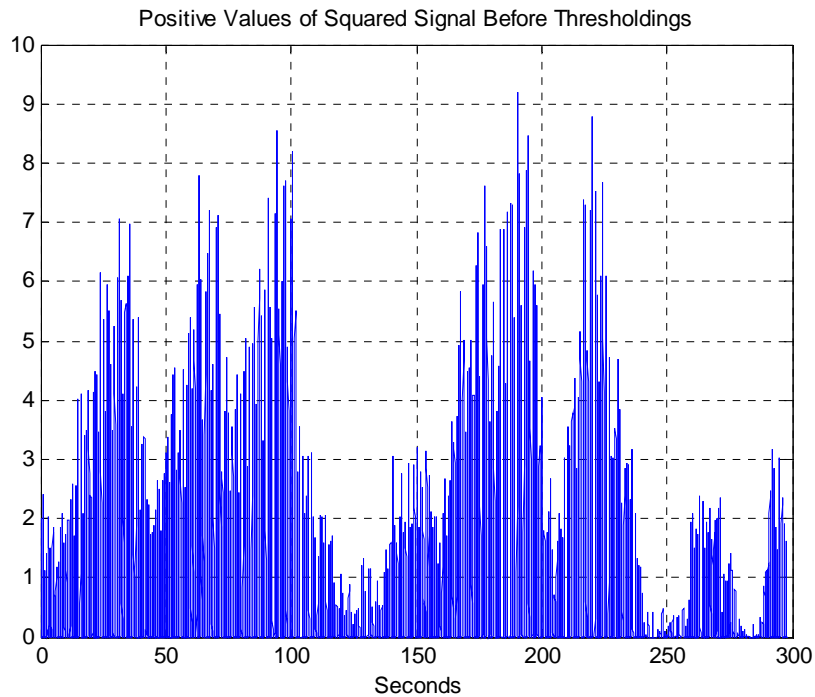


Figure 3.12: Signal after Clipping Negative Amplitudes and Squaring Positive Parts.

Once the non-positive values have been eliminated, a zero-crossing method, based on the derivative of the signal, was then used to detect the locations of the peaks. Only large amplitude parts of the squared signal were considered when looking for zero-crossings of the derivative to be declared beat peaks. While using the zero-crossing method we also used a parameter  $Q$  which assures that there is a certain minimum distance between two peaks. This allowed us to get rid of

the peaks that were too close to be actual peaks that correspond to heart beats. Figure 3.13 shows an example of the locations where beat peaks were found.

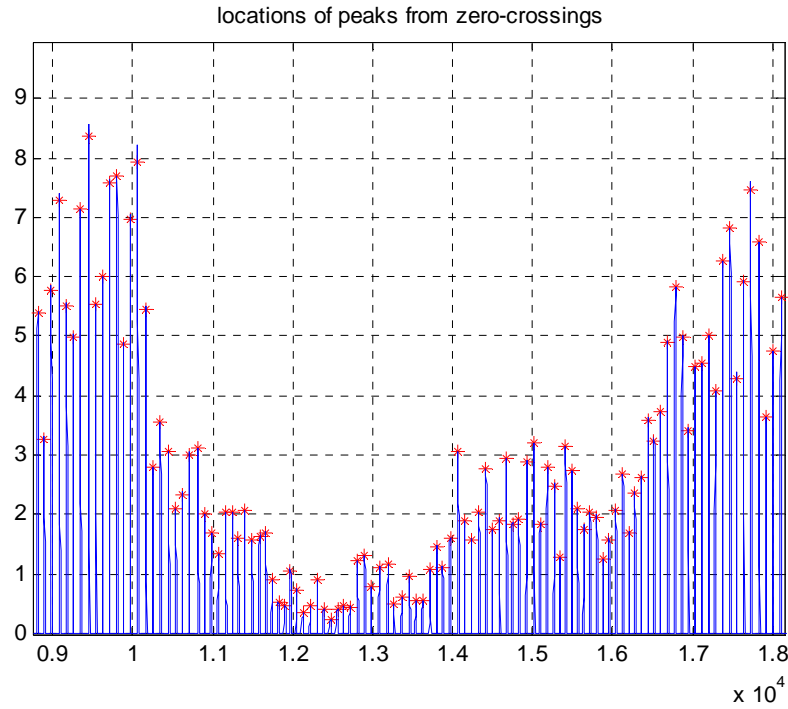


Figure 3.13: Determination of Locations of Peaks Using Zero Crossings of Derivatives

In the peak detection, we also used a smart thresholding step to further eliminate invalid peaks. In general, thresholding operation is performed as a global or as a variable step.

### 3.4.1 Global Thresholding

This thresholding technique just uses one threshold value and ignores all the peaks below or above it as specified by the user. This is not a good thresholding technique as the amplitude of the squared signal changes a lot therefore one threshold value cannot provide the desired result [18]. Lots of peaks could not be detected using this thresholding technique when it was evaluated.

### 3.4.2 Variable Thresholding

Variable thresholding is an ideal approach to detect beat peaks and discard all other invalid peaks. Variable thresholding is a time varying approach where the amplitude of the threshold keeps changing according to the local, average amplitude of the signal or a similar quantity based on previously detected peaks [18]. By employing the first approach we were able to reduce the number of missed peaks significantly compared to what we would get using global thresholding. Figure 3.14 shows an example of variable thresholding and actual peaks that were detected as a result of this thresholding. The blue line is the squared signal, the red line shows the local threshold that was used to decide where to look for beat peaks (above this line), and the green vertical lines show the locations of the beat peaks that were found.

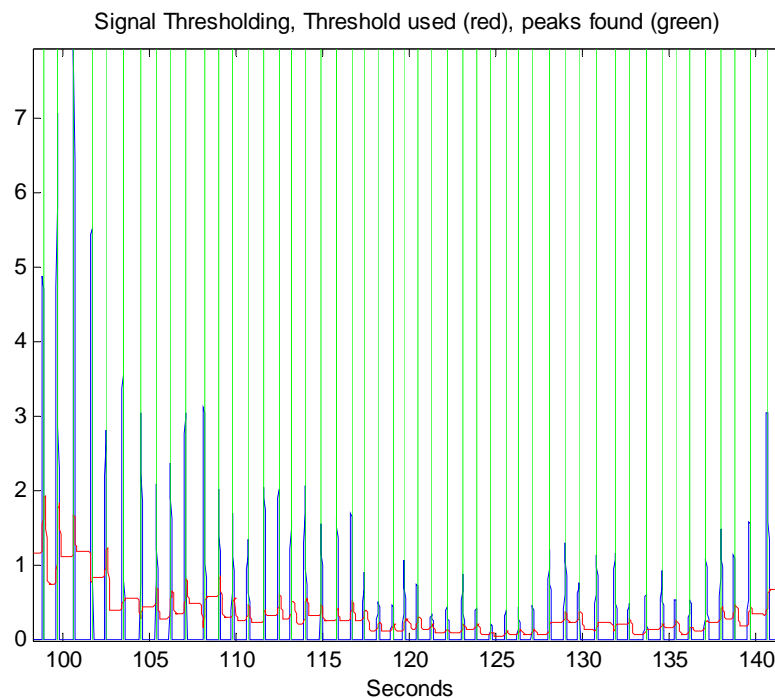


Figure 3.14: Variable Thresholding Using Time Varying Threshold

### **3.5 Peak-to-Peak (P-P) Interval Detection**

The peak finding step gives all the indices where a beat peak was obtained. The peak-to-peak intervals signal is then obtained as the successive difference of the sample indices associated with the peaks divided by the sampling frequency. Mathematically, the peak-to-peak interval sequence (in units of seconds) is given as:

$$PP(n)=(P(n)-P(n-1))/F_s$$

where  $P(n)$  is the  $n^{\text{th}}$  location of a beat peak.

### **3.6 P-P Outliers (Missed Peaks) Detection and Smoothing Scheme**

The peak-to-peak or Peak-Peak (P-P) interval signal plays a very important part in deriving the HRV signal through a non-uniform interpolation technique and this signal plays a key role in estimating the state of the Autonomic Nervous System (ANS). Thus, detecting the correct intervals is very important. Therefore we incorporated a scheme in our algorithm that automatically checks if there have been any P-P interval outliers, and if so it uses a moving average filter to correct them to prevent HRV signal corruption. The moving average filter keeps track of the P-P intervals and uses the value equal to the local average of the past  $N$  and next  $N$  P-P intervals to replace the locations where a missed peak was detected. A typical value used for  $N$  is 5. An outlier is declared if any P-P interval is 1.5 times greater than the local average of the P-P intervals. An outlier is replaced with the local average of P-P intervals. Thus, this technique smooths the P-P interval outliers. Previous researchers have also incorporated automatic correction schemes to produce better results than manual editing to correct the signal [1].

Figures 3.15 and 3.16 are examples of P-P outlier detection and smoothing.

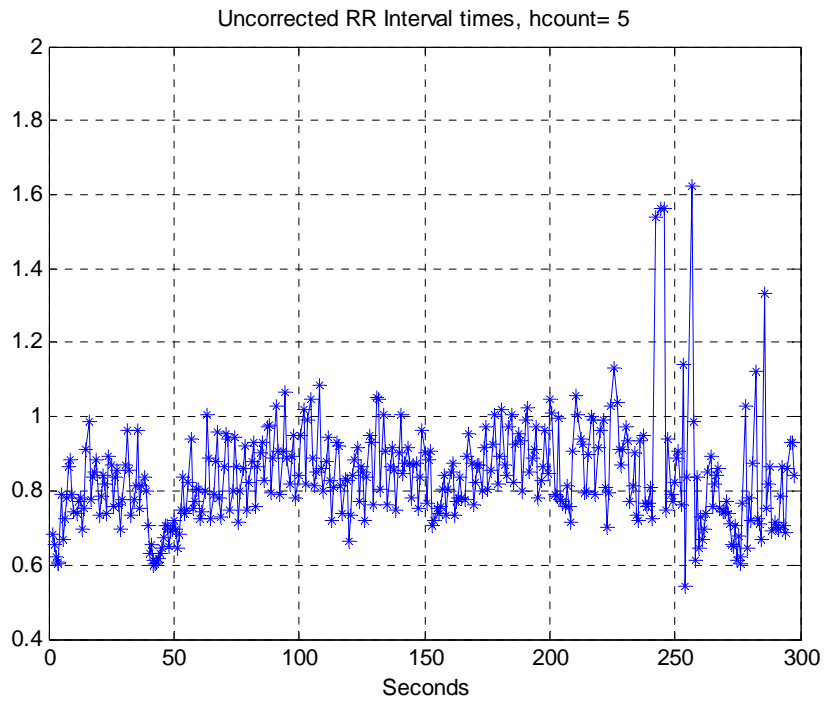


Figure 3.15: Signal with Missed Peaks

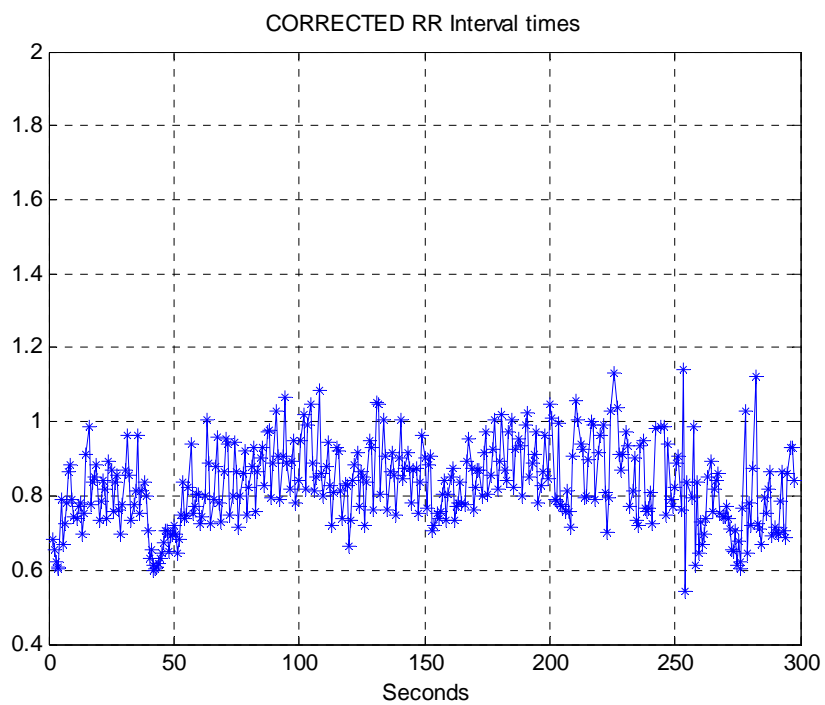


Figure 3.16: Corrected Signal Using Moving Average Filter

The corrected Peak-Peak intervals signal is then used to perform Time-Domain Analysis. Time most commonly used time-domain analysis is to compute simple statistics, such as mean and standard deviation, of the P-P intervals. Also Peak-Peak interval signal is used to compute an average Heart Rate over a period of time. An instantaneous Heart Rate can be obtained as

$$HR = 60. / (P-P \text{ Intervals});$$

in the units of beats per minute. We also performed a histogram generation operation of P-P and HR because it is useful to visualize their spread. Figure 3.17 and 3.18 shows two such histograms.

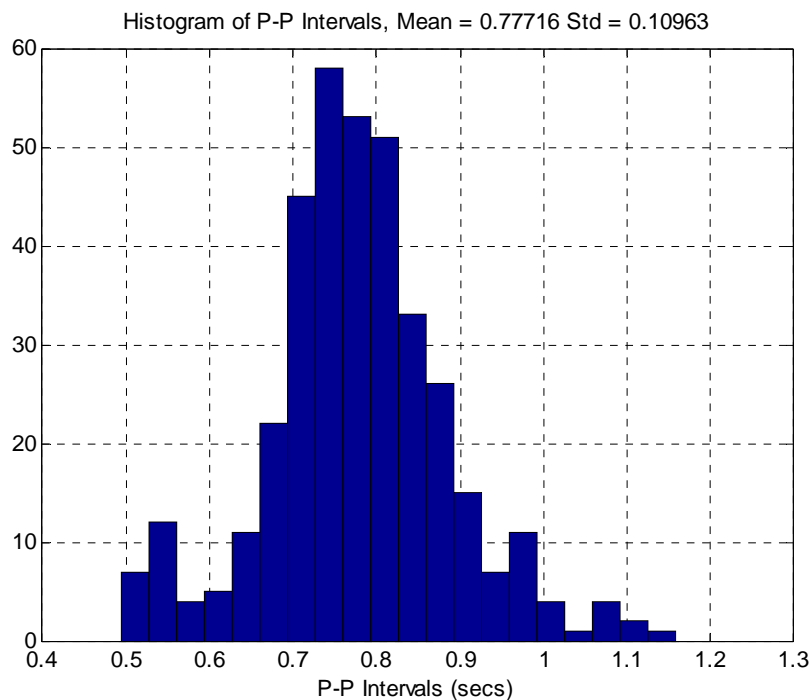


Figure 3.17: Histogram of Peak-Peak interval Signal

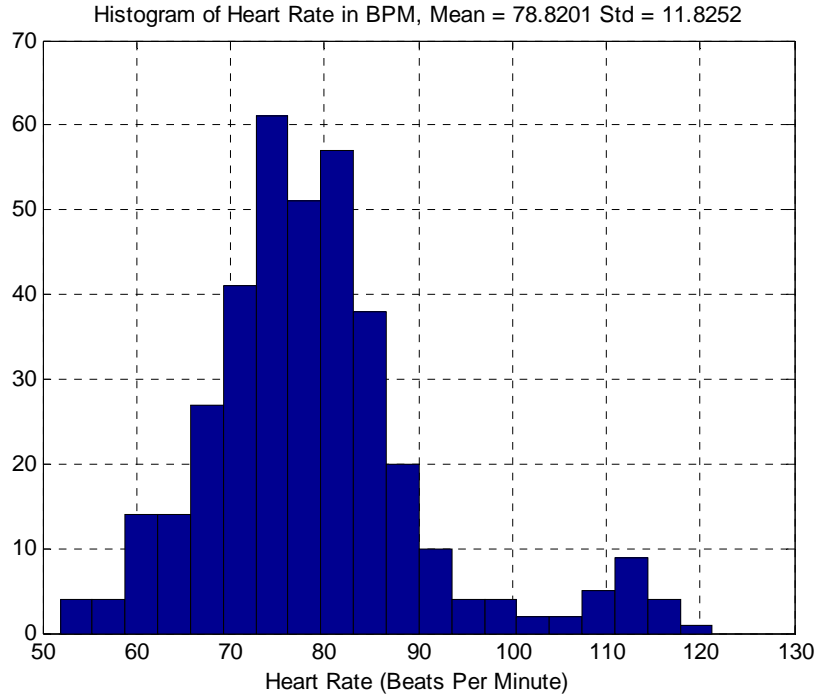


Figure 3.18: Histogram of Instantaneous Heart Rate

### 3.7 Heart Rate Variability Signal Derivation

After obtaining Peak-Peak intervals we used interpolation techniques to obtain a Heart Rate Variability (HRV) signal that is a function of time. We explored various interpolation schemes available in Matlab such as cubic splines, linear, nearest neighbor, etc. To perform the interpolation operation we used the Matlab command `interp1`. An example of a command that performs the (non-uniform) interpolation operation has the format as follows:

$$V_q = \text{interp1}(X, V, X_q, \text{METHOD}, \text{EXTRAVAL})$$

Where,

$V_q$  = resultant interpolated signal

X= locations where a peak was found

V= values of the P-P interval signal at the peak locations,

Xq= locations where the HRV signal is desired (query points) which is typically a uniform set of time locations

Method= cubic, linear, nearest, piecewise

Extraval= value given to interpolation results outside of the range of X which would otherwise result in 0 or an undefined value (NaN).

A HRV signal which is obtained as a result of above explained operation with the nearest neighbor method is shown in figure 3.19.

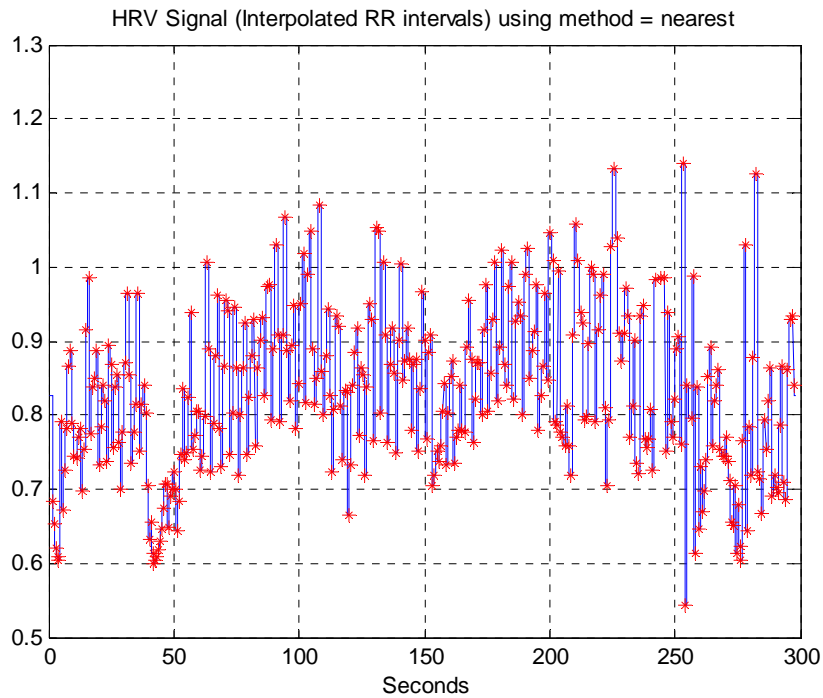


Figure 3.19: Derived HRV Signal Using Nearest Neighbor Interpolation Technique

Also, figures 3.20 and 3.21 show a reduced time range of the HRV signal to show the comparison of two interpolation schemes that are used to generate the HRV signal. The cubic spline method tends to give a smoother connection of points compared to the linear (not shown) or nearest neighbor methods.

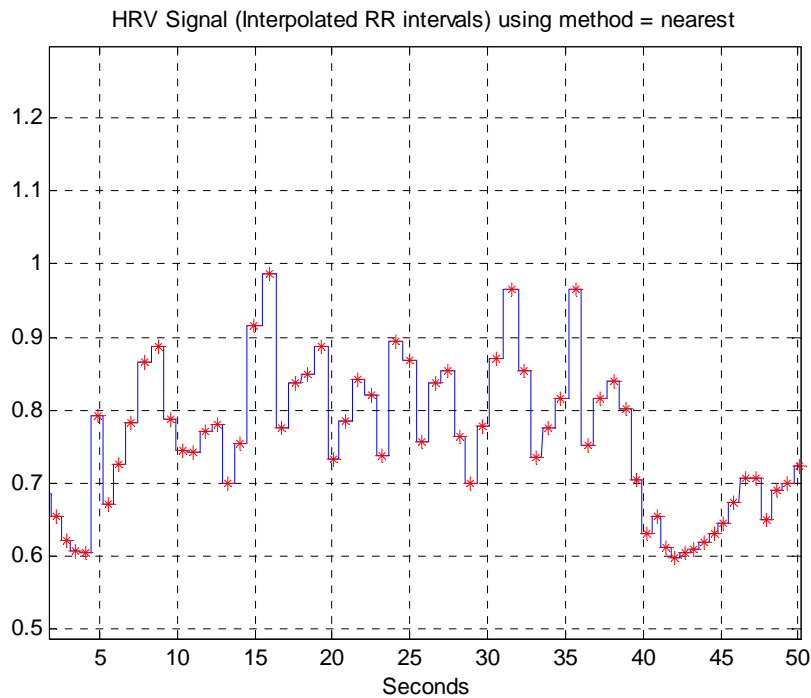


Figure 3.20: Example of HRV Derivation Using Nearest Method

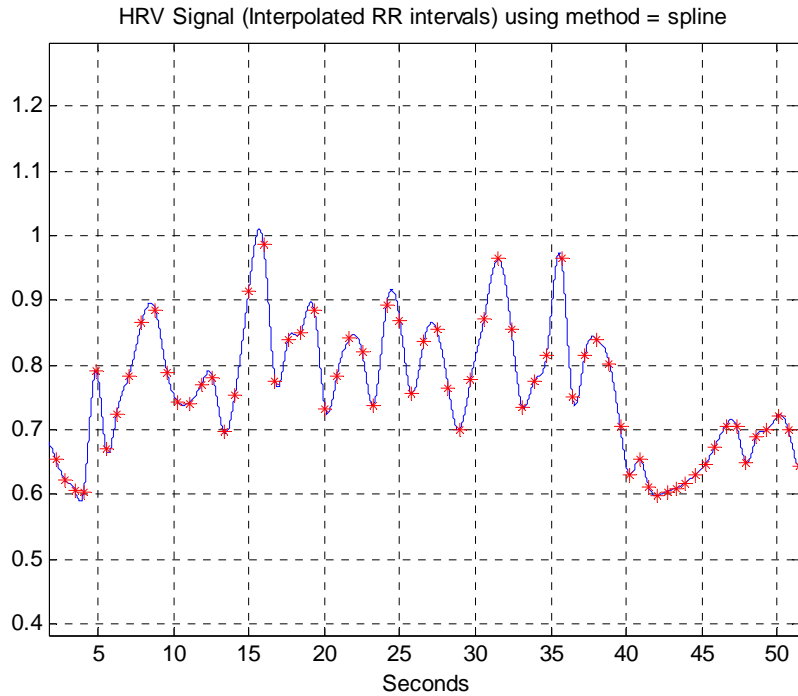


Figure 3.21: Example of HRV Derivation Using Cubic Spline Method

Figures 3.22 and 3.23 are two example spectra of an HRV signal generated using the spline and nearest neighbor methods. Based on empirical results we found that spline interpolation techniques gives the lowest LF/HF ratio compared to nearest neighbor and linear methods. Between the linear and nearest neighbor methods, the high frequency information is guaranteed to be lower for linear interpolation which produces a higher LF/HF ratio.

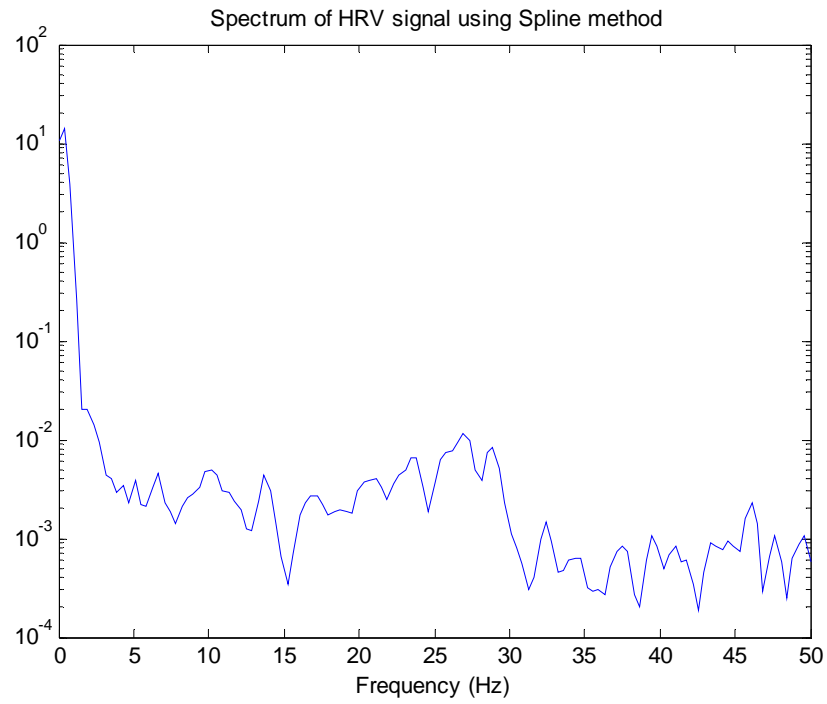


Figure 3.22: Spectrum of HRV Using Cubic Spline Method

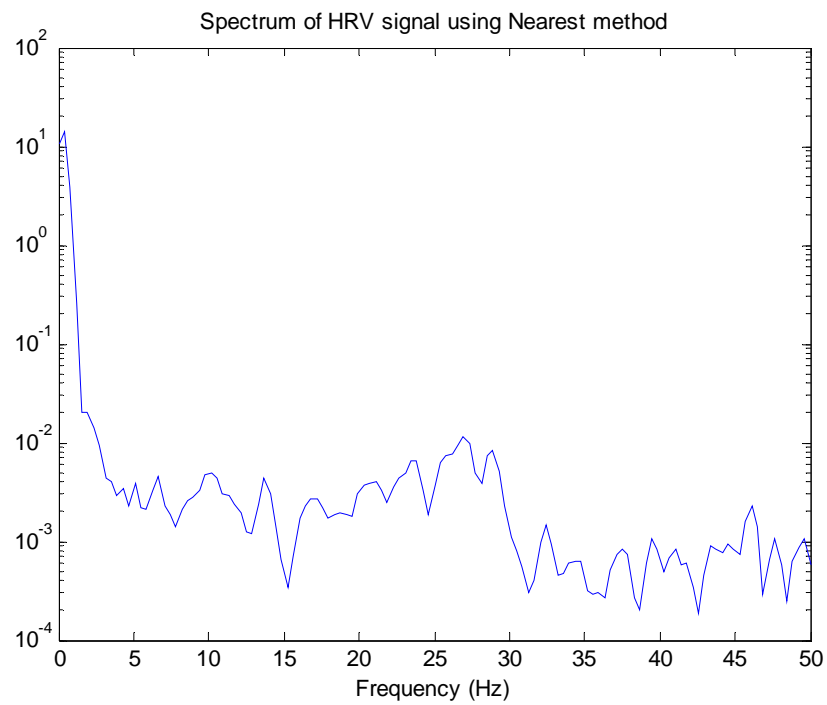


Figure 3.23: Spectrum of HRV Using Nearest Method

Table 3.1 shows the low frequency to high frequency (LF/HF) ratio that we obtain using various interpolation schemes and the non-parametric method of spectrum estimation.

Data	Nearest	Linear	Spline
Data1	1.88	2.2	1.61
Data2	1.26	1.49	1.09
Data3	2.5	2.97	2.13
Data4	1.83	2.41	1.78
Data5	2.53	2.87	2.23
Data6	1.05	1.18	0.93
Data7	1.16	1.38	1.09
Data8	1.32	1.63	1.08
Data9	2.05	2.44	1.76
Data10	1.6	1.96	1.39
Data11	2.06	2.54	1.69
Data12	2.86	3.44	2.42
Data13	1.19	1.4	1.02
Data14	0.94	1.14	0.8
Data15	0.87	0.99	0.77
Data16	2.72	3.09	2.4
Data17	2.68	3.03	2.41
Data18	1.73	2.05	1.5
Data19	1.82	2.09	1.64
Data20	0.89	1.02	0.8
Mean	1.74	2.06	1.52
STD	0.65	0.76	0.57

Table 3.1: Comparison of Interpolation Results (LF/HF Ratio) Using Non-Parametric Spectral Estimation

Table 3.2 shows the low frequency to high frequency (LF/HF) ratio that we obtain using various interpolation schemes and the parametric method of spectrum estimation.

Data	Nearest	Linear	Spline
Data1	1.88	2.16	1.59
Data2	1.27	1.5	1.08
Data3	2.52	2.93	2.13
Data4	1.73	2.29	1.68
Data5	2.79	3.19	2.48
Data6	1.29	1.43	1.1
Data7	1.38	1.7	1.3
Data8	1.39	1.76	1.13
Data9	2.13	2.56	1.81
Data10	1.63	2.02	1.39
Data11	2.12	2.63	1.74
Data12	2.57	3.08	2.18
Data13	1.27	1.53	1.06
Data14	0.88	1.07	0.74
Data15	0.87	0.95	0.74
Data16	2.69	3.16	1.55
Data17	2.55	2.85	2.31
Data18	1.73	2.03	1.5
Data19	2.16	2.44	1.88
Data20	0.99	1.11	0.86
Mean	1.79	2.11	1.51
STD	0.62	0.72	0.51

Table 3.2: Comparison of Interpolation Results (LF/HF Ratio) Using Parametric Spectral Estimation

### 3.8 Downsampling HRV Signal

Since the original PPG signal was sampled at a very high rate, it is very important to resample it at lower rate before doing any spectral analysis. This is mainly because the frequency content of interest in an HRV signal is limited to very a very low frequency range (less than 0.5 Hz). However, if a spectral analysis has to be done on a signal that is sampled at a high rate, a very long window size would have to be used which makes the process computationally inefficient. By resampling the HRV signal to a lower rate, we were able to study the spectral features using a

small window size. Before decimating the HRV signal its spectrum was calculated to determine the essential bandwidth of the signal to see if anti-aliasing filtering was required for a severe downsampling of the signal. Figure 3.24 shows a typical spectrum of an HRV signal before downsampling.

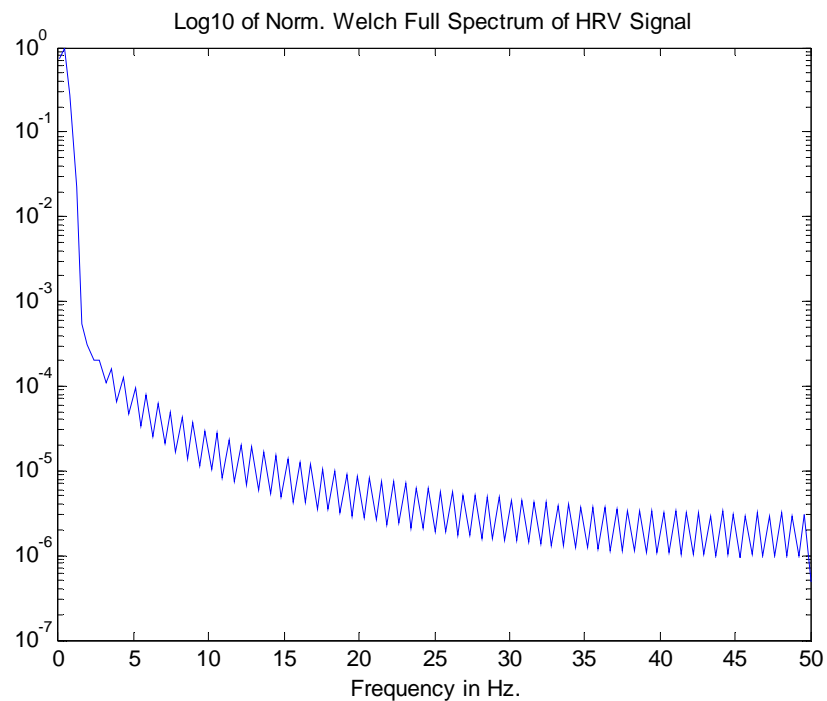


Figure 3.24: Welch Full Spectrum of HRV before Downsampling

From spectrum above we declared the bandwidth of the signal to be about 3Hz. To resampled the signal down to 2 SS for an efficient spectral analysis, we used an anti-aliasing filter.

To severely downsample the HRV signal this way, we used a Matlab command as shown below:

$$Y = \text{decimate}(X, R, \text{'FIR'})$$

Where,

Y=Decimated signal

X=Signal to be decimated

$R$ =Factor by which signal has to be decimated (an integer)

$FIR$ =length of an FIR filter to be used for anti-aliasing filtering.

A severely downsampled HRV signal is shown in figure 3.25:

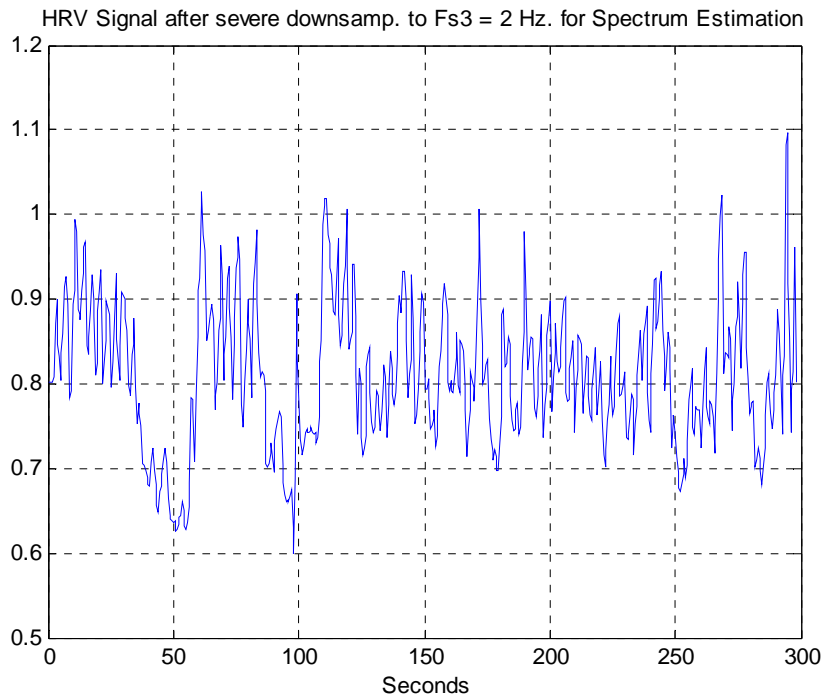


Figure 3.25: HRV Signal after Severe Downsampling

### 3.9 Frequency Domain Analysis

As mentioned earlier, frequency domain analysis techniques are used to generate the spectrum of the HRV signal to study the balance of Autonomic Nervous System. In approach which follows [2] we incorporated two different spectrum estimation techniques i.e. Non Parametric and Parametric.

### 3.9.1 Non Parametric Method

For non-parametric spectral estimation we used the Welch method. Welch method splits the data into overlapping segments and compute its modified Periodogram of each segment and then averages the results to produce power spectral density estimate.

Each of the overlapping segments is first windowed using Hamming window or by any user defined window. The size of the window and the degree of overlap are defined by the user. The simplest use of the function in Matlab that computes non-parametric spectral estimates is explained below;

$$[P_{xx},w] = pwelch(x,window)$$

Where  $P_{xx}$  is the vector of values of the Power Spectral Density (PSD) of the signal  $x$  using the Welch method and a window of type and size defined by the user and whose values are in the vector with the same name. The vector  $w$  has the associated frequency values where  $P_{xx}$  is defined. Figure 3.26 shows a PSD of signal determined using Welch method and a Hamming window of size 128.

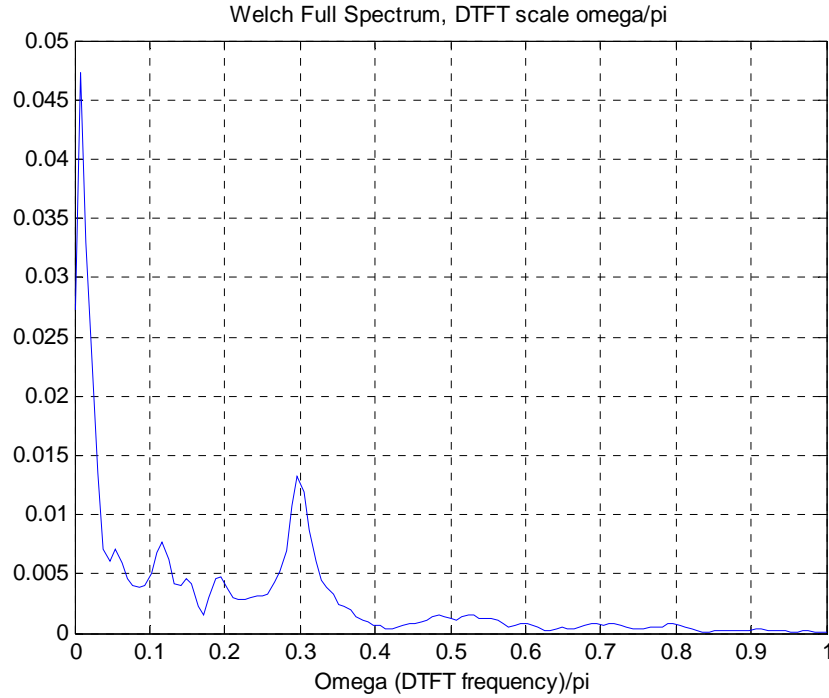


Figure 3.26: Welch Full Spectrum of HRV after Severe Downsampling

The PSD is calculated in the units of power vs. radians per sample. However we are interested in calculating frequency in units of Hz for our research. Therefore, the frequency scale was normalized to give power between 0-1 Hz. as shown in figure 3.26.

Finally, we were interested in computing the power in the frequency range that corresponds to Sympathetic Nervous System and Parasympathetic nervous System. Thus we divided the estimated Welch PSD into low (0.04-0.15 Hz) and high frequency (0.15-0.4 Hz) regions. The total area under these two regions were computed and then the ratio of two regions to estimate the balance of Autonomic Nervous System. Figure 3.27 shows an example of such estimation:

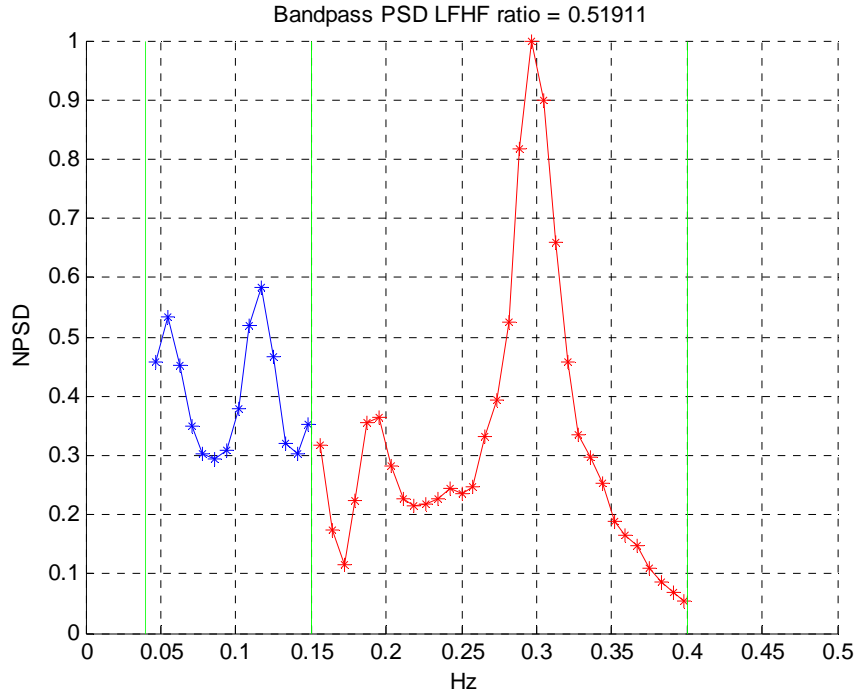


Figure 3.27: Non-Parametric Spectrum of HRV Signal

The area under the red region is total high frequency power and it corresponds to the Parasympathetic Nervous System. The area under the blue region is the total low frequency power and it corresponds to the Sympathetic Nervous System.

### 3.9.2 Parametric Method

For parametric spectral estimate of the HRV signal we used the Burg method of Auto-Regressive (AR) spectrum estimation with specified order.

Figure 3.28 shows full spectrum of an HRV signal obtained using the Burg method using an order of 16.

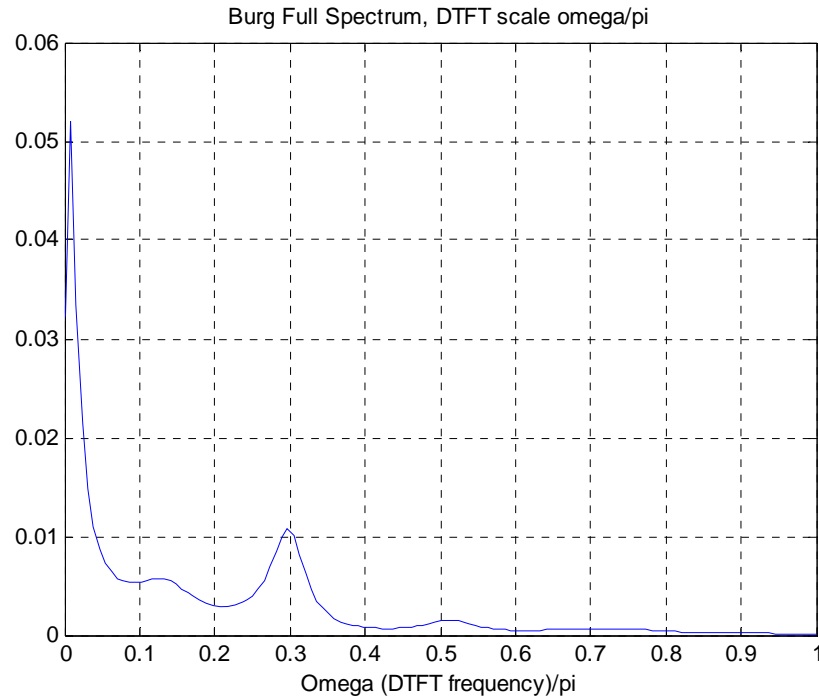


Figure 3.28: Burg Full Spectrum of HRV Signal

To obtain the estimate of the balance of Autonomic Nervous System the spectrum has to be divided into low frequency and high frequency regions as it was done while computing the estimate using the Welch spectrum.

An example of such an estimate using AR modeling is shown in figure 3.29 with model order 16 as suggested in [2].

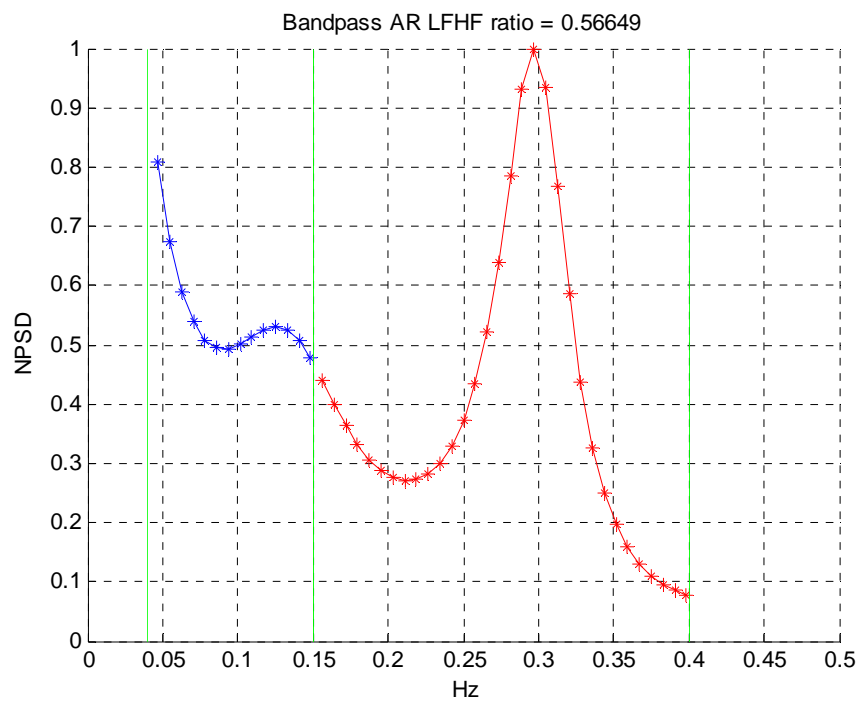


Figure 3.29: Parametric Spectrum HRV Signal

## **Chapter 4**

### **Time Domain Analysis**

In this chapter various time domain techniques used in ECG/PPG signal analysis will be discussed in detail.

#### **4.1 Time Domain Analysis**

Time domain analysis techniques performed on ECG/PPG signals is often referred to as simplest way of analyzing such signals. Depending upon the length of the recording, the time domain analysis technique can be divided into long term and short term time domain analysis.

##### **4.1.1 Long Term Recording**

Long term recording involves collection of data for 24 hours or more. The various time domain parameters that are used to analyze long term recordings are instantaneous heart rate, comparison between night time and day time heart rate, average heart rate over a period of recording, standard deviation of heart rate over a period of recording, average of peak-to-peak intervals, successive difference of peak-to-peak intervals, standard deviation of peak-to-peak intervals, NN50 count, pNN50 value, etc. [2].

However, for the purpose of this research we did not analyze any long term signals.

##### **4.1.2 Short Term Recording**

Short term recordings are recording of signals over 5 to 10 minutes in length. For this research we used a variety of short term recordings for time domain analysis to estimate the mental status of a subject. The various time domain parameters that we incorporated in this algorithm are

histogram of heart rate, histogram of peak-to-peak interval, histogram of successive differences of peak-to-peak intervals, average heart rate, average peak-to-peak interval, root mean square of successive difference of peak-to-peak intervals, NN50 count and pNN50 value [2].

To perform time domain analysis, short term recording was done on three different groups which were relaxed (medicated), normal (un-medicated) and (presumably) stressed. In following sections we will show results of time domain analysis performed on these three groups.

#### 4.2 Time Domain Analysis on Relaxed Person (Medicated)

All the results of analysis which we show in this section were performed on a signal which was 5 minutes in length. Figures 4.1-4.3 show histograms of heart rate, peak-to-peak (P-P) interval and successive differences of P-P intervals (in units of seconds) for a signal that belongs to a relaxed (medicated) case.

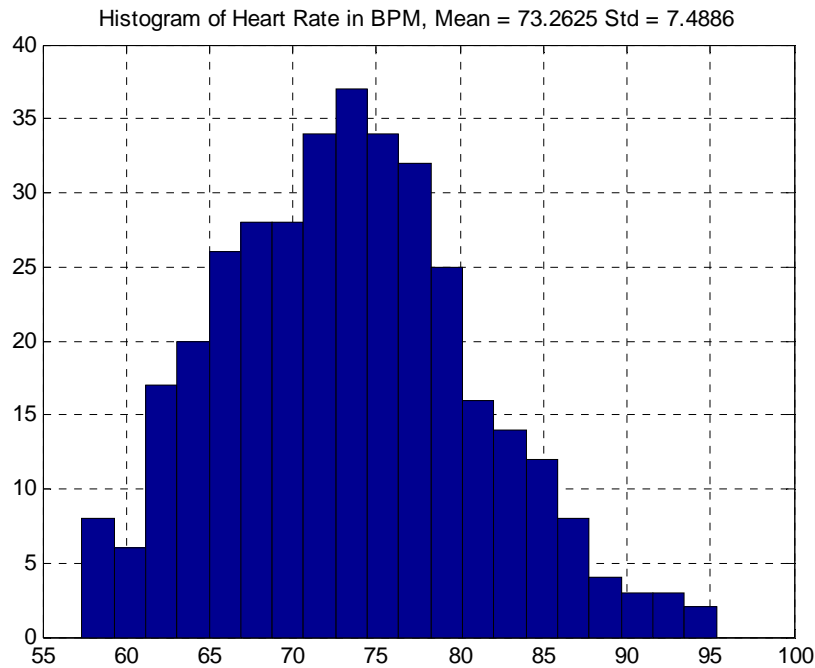


Figure 4.1: Histogram of Heart Rate of Relaxed Subject

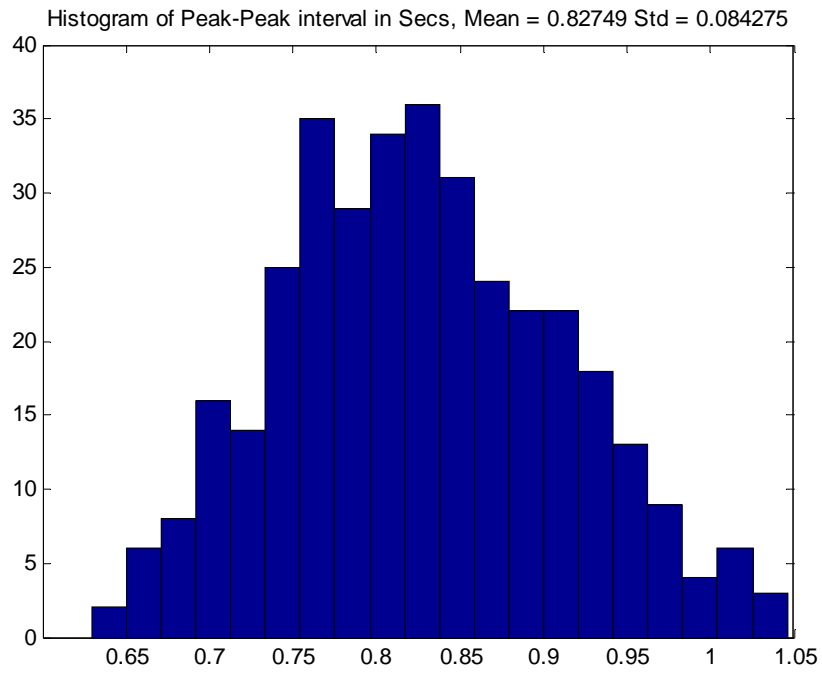


Figure 4.2: Histogram of Peak-Peak interval of Relaxed Subject

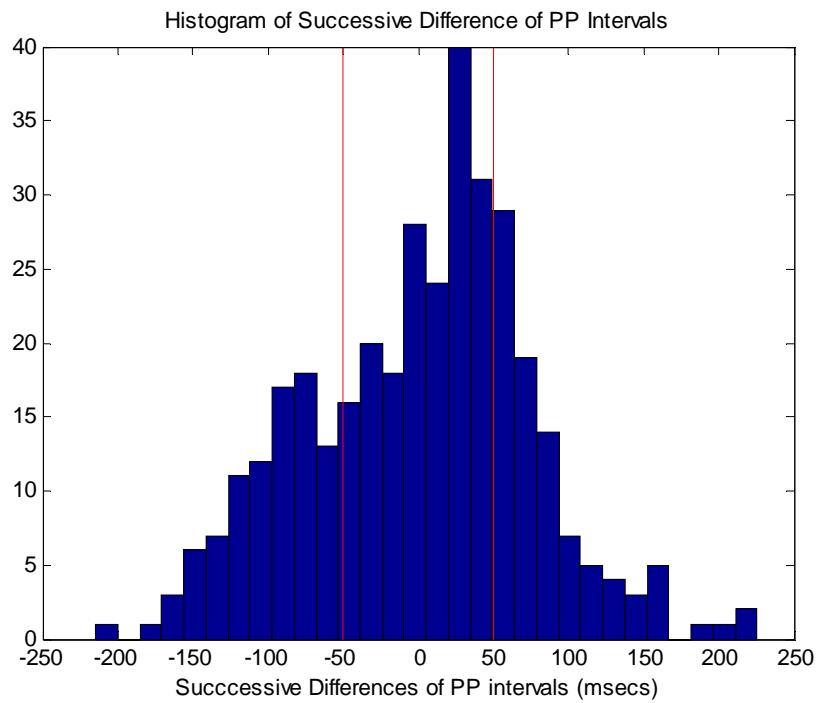


Figure 4.3: Histogram of Successive Differences of Peak-Peak interval

Table 4.1 shows the combined compiled results of analysis of various time domain parameters for the relaxed (medicated) subject case. Results show relatively consistent numbers for all 6 recordings considered to illustrate this case.

Data	Mean HR	STD HR	RMSSD	NN50	pNN50	Mean P-P	STD P-P
Data100	72.2	7.23	0.074	222	63.06	0.83	8.54
Data101	75.63	8.12	0.072	205	55.7	0.8	8.63
Data102	74.19	9.01	0.09	232	64.44	0.82	10.06
Data103	73.84	10.07	0.11	247	69.77	0.82	11.04
Data104	76.31	9.3	0.08	229	61.72	0.79	9.52
Data105	78.82	11.82	0.1	239	64.42	0.77	10.96
Mean	75.16	9.36	0.08	229	63.18	0.8	9.79
STD	2.29	1.37	0.01	14.54	4.57	0.02	1.09

Table 4.1: Results of Various Time Domain Parameters for Relaxed Subject

### 4.3 Time Domain Analysis on Normal Person (Un-medicated)

Figures 4.4-4.6 show histograms of heart rate, peak-to peak-interval and successive difference of P-P intervals (in units of seconds) of a signal of that belongs to un-medicated case.

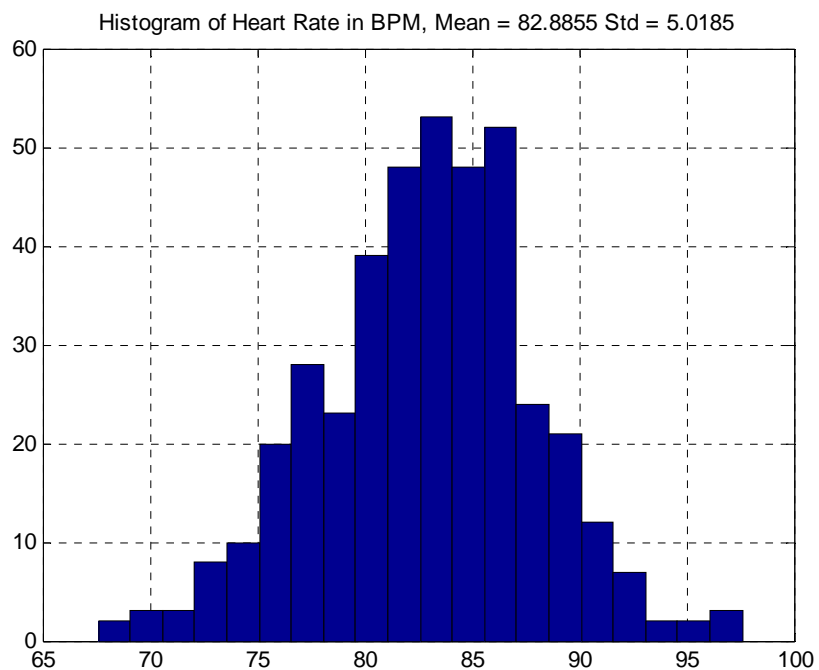


Figure 4.4: Histogram of Heart Rate of a Normal Subject

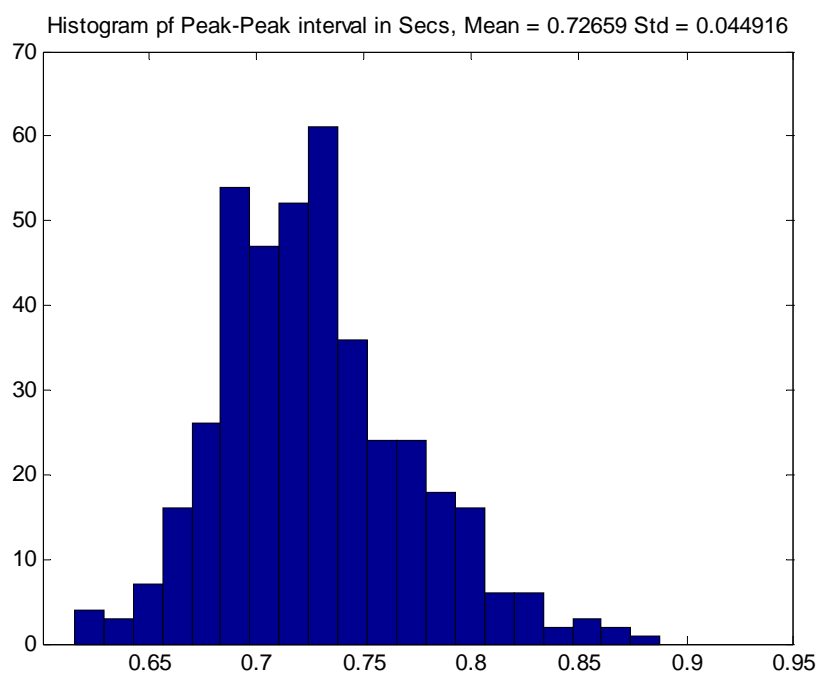


Figure 4.5: Histogram of Peak-Peak interval of Normal Subject

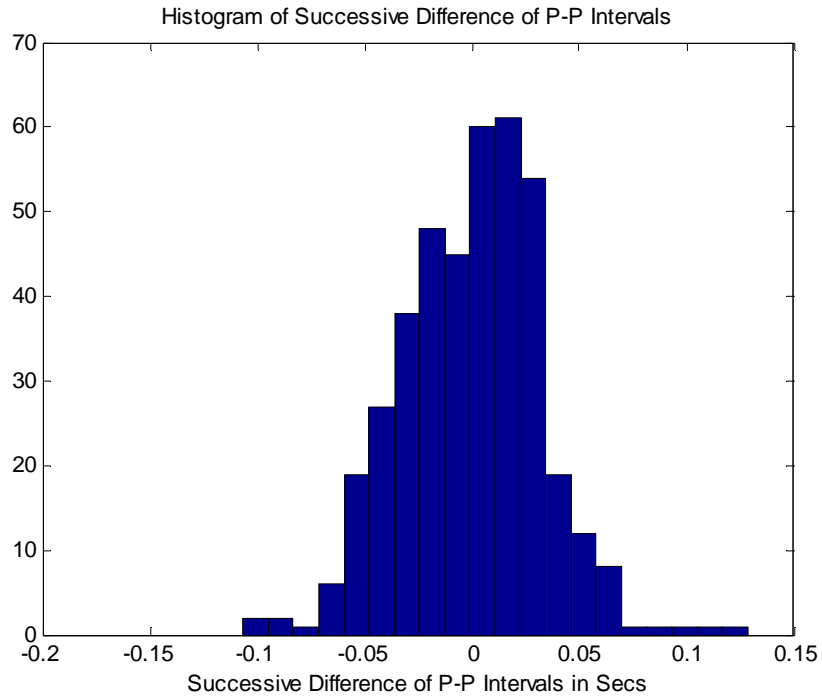


Figure 4.6: Histogram of Successive Differences of Peak-Peak intervals

Table 4.2 shows combined compiled results of various time domain analysis parameters for this case. Again, results show relatively consistent numbers for all 6 recordings considered to illustrate this case.

Data	Mean HR	STD HR	RMSSD	NN50	pNN50	Mean P-P	STD P-P
Data110	82.88	5.01	0.074	121	29.72	0.72	4.49
Data111	80.9	5.63	0.03	108	27.2	0.74	5.35
Data112	79.92	5.97	0.03	137	34.86	0.75	5.54
Data113	80.59	6.33	0.03	133	33.67	0.74	5.7
Data114	77.88	5.89	0.04	156	40.83	0.77	5.87
Data115	76.18	5.94	0.04	183	48.93	0.79	6.3
Mean	79.72	5.79	0.04	139.66	35.86	0.75	5.54
STD	2.37	0.44	0.01	26.63	7.92	0.02	0.6

Table 4.2: Results of Various Time Domain Parameters for Normal Subject

#### 4.4 Time Domain Analysis on Stressed Person

Figures 4.7-4.9 show histograms of heart rate, peak-to-peak interval and successive differences of P-P intervals (in units of seconds) respectively for one signal that belongs to a stressed subject case.

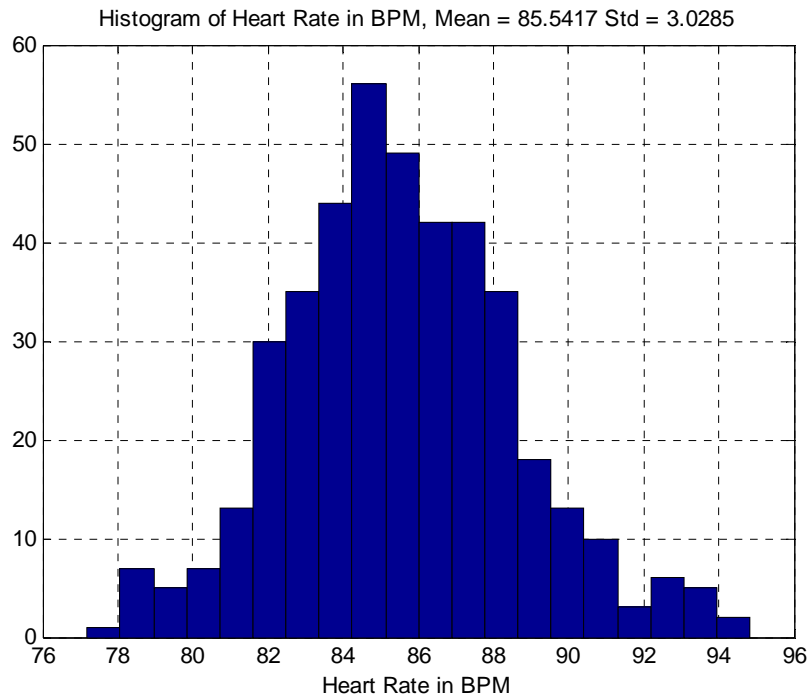


Figure 4.7: Histogram of the Heart Rate of a Stressed Subject

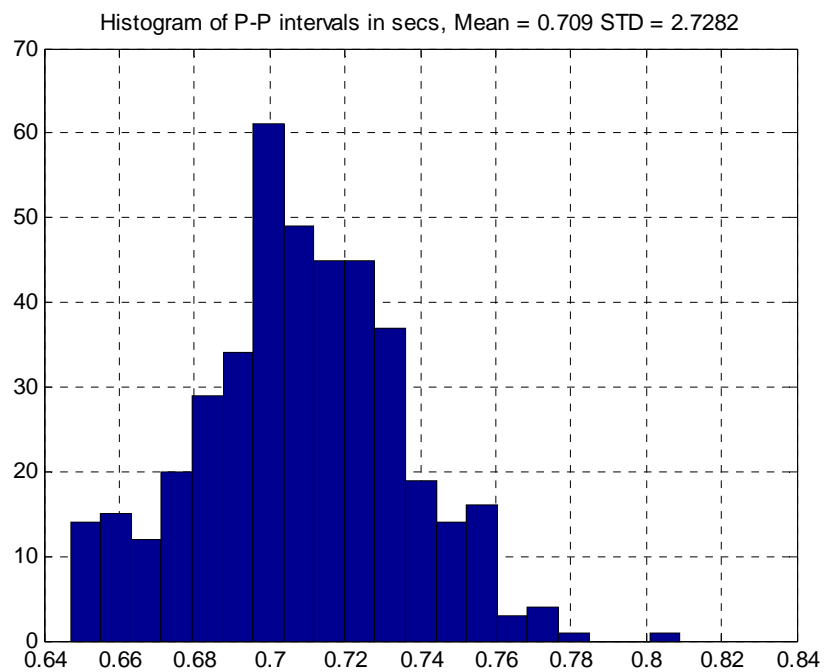


Figure 4.8: Histogram of the P-P Intervals of a Stressed Subject

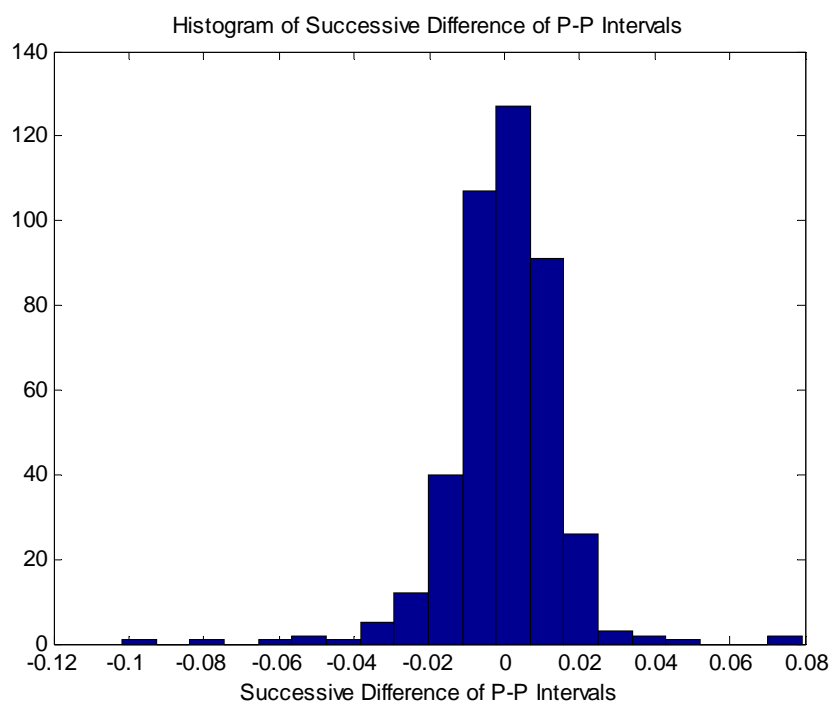


Figure 4.9: Histogram of Successive Differences of Peak-Peak interval

Table 4.3 shows combined compiled result of analysis of various time domain parameters for this case. The results still show relatively consistent numbers for the 6 recordings; however, more consistency is noted for the first 4 recordings considered to illustrate this case.

Data	Mean HR	STD HR	RMSSD	NN50	pNN50	Mean P-P	STD P-P
Data116	84.96	3.74	16.11	15	3.58	0.7	3.17
Data117	82.42	5.49	31.41	13	3.21	0.73	3.68
Data118	85.54	3.02	15.04	14	3.31	0.7	2.47
Data119	84.85	3.27	13.88	13	3.11	0.7	2.72
Data120	67.7	4.15	0.06	46	13.85	0.88	4.77
Data121	68.1	4.18	0.04	19	5.72	0.86	5.14
Mean	78.92	3.97	12.75	20	5.46	0.76	3.65
STD	8.61	0.87	11.73	12.93	4.22	0.08	1.09

Table 4.3: Results of Various Time Domain Parameters for Stressed Subject

## **CHAPTER-5**

### **Frequency Domain Analysis and Algorithm Validation**

To verify the algorithm we recorded PPG signals while making the subject experience different environmental and mental conditions and the response of the subject was studied by analyzing frequency domain features. All recorded data that we used were 5 minutes in length. We found very different results as a consequence of using different conditions. We employed both Parametric and Non-Parametric frequency domain analysis technique and the results were in agreement with each other.

The various conditions that we used to stimulate different conditions were: (1) using a nano patches, (2) recording signal after an intense work out session, and (3) using blue enriched light to study their effects on the Autonomic Nervous System.

#### **5.1 Nano-Scale Patch**

There are nano-scale patches that are used to stimulate appropriate acupuncture points and thus their application is expected to relax a subject. The nano-scale patch used here is designed by Lifewave, is very convenient to apply, and it starts showing effects as early as 15 minutes after its application [30].

Figures 5.1-5.4 show information about the patches and their proper location for their application on the human body.

Figures 5.1-5.4 show the patches its description and position of application of nano scale patch.



Figure 5.1: Y-age Relaxation Patches Packet [31]



Figure 5.2: Relaxation Patches

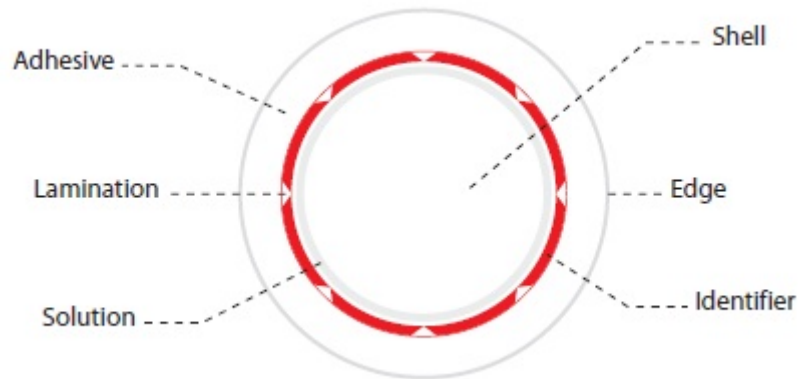


Figure 5.3: Labeled Explanation of a Patch [32]



Figure 5.4: Location of Application of Patch on a Body [30]

Since the patches are expected to reduce the stress, we are expected to show more power in the high frequency region of the HRV signal spectrum i.e. dominance of the Parasympathetic ANS. Figures 5.5 and 5.6 are examples of parametric and non-parametric HRV spectra on a normalized scale generated from a signal collected using the nano-scale patch.

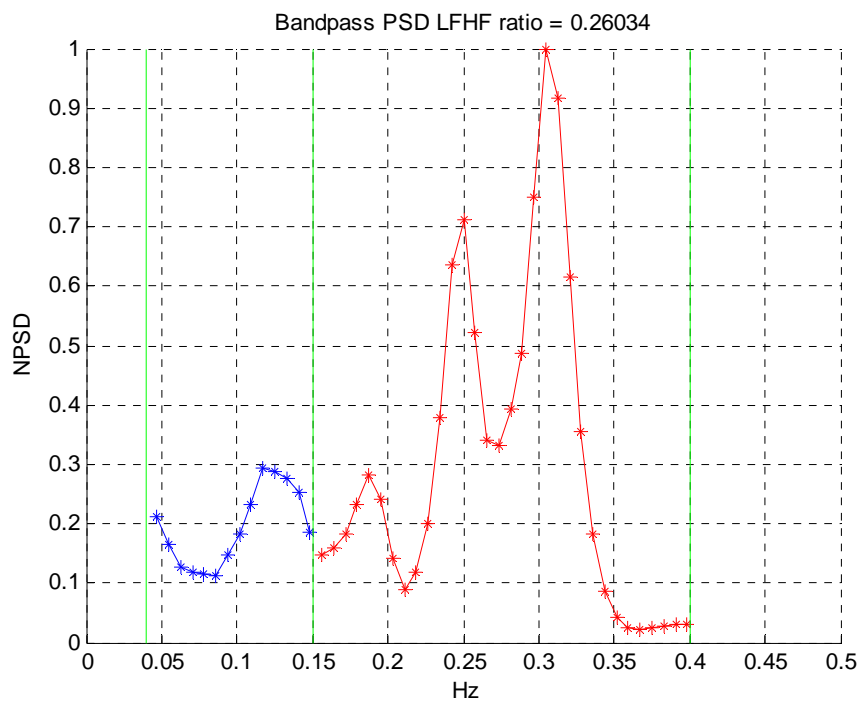


Figure 5.5: Welch Spectrum of a Relaxed Subject

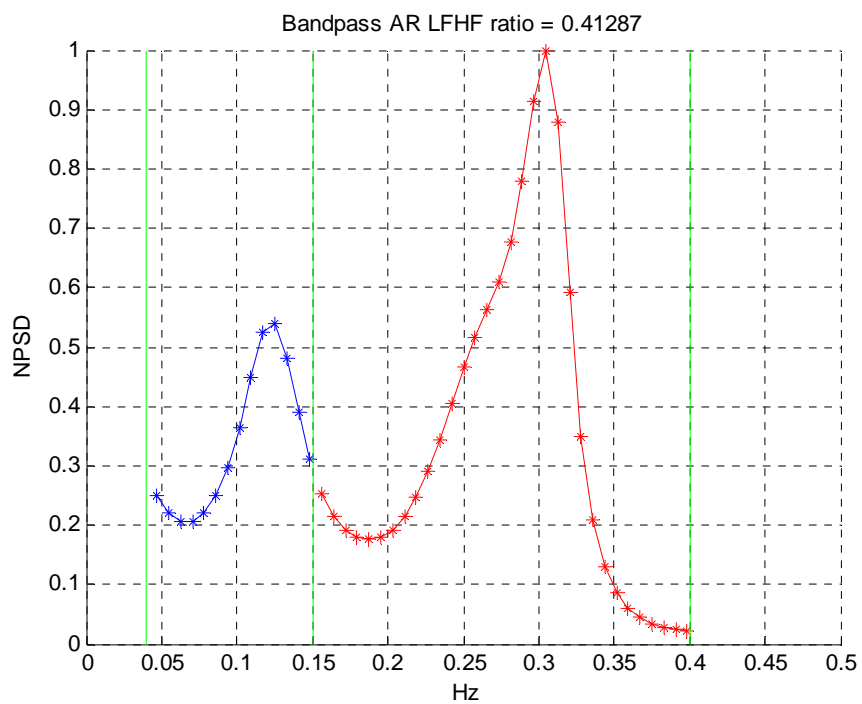


Figure 5.6: AR Spectrum of a Relaxed Subject

Table 5.1 and Table 5.2 show a collection of experimental frequency domain results obtained by analyzing signals which were recorded using the nano-scale patches. Both methods used to produce the PSD estimate give similar results with the parametric methods producing a slightly higher average LF/HF ratio. All parametric PSD estimates are obtained using the recommended model order of 16 [2].

Data	LF (n.u)	HF (n.u)	LF/HF (FFT)
Data 200	0.473	0.527	0.8974
Data 201	0.5395	0.4605	1.1718
Data 202	0.2066	0.7934	0.2603
Data 203	0.3417	0.6583	0.5191
Data 204	0.2833	0.7167	0.3953
Data 205	0.535	0.465	1.1507
Data 206	0.5205	0.4795	1.0855
Data 207	0.4984	0.5016	0.9938
Data 208	0.3435	0.6565	0.5233
Mean	0.4157	0.5843	0.7775
STD	0.1238	0.1238	0.3528

Table 5.1: Results of Frequency Domain Analysis Using Patches and FFT Method

Data	LF (n.u)	HF (n.u)	LF/HF (AR)
Data 200	0.4776	0.5224	0.9144
Data 201	0.5378	0.4622	1.1636
Data 202	0.2922	0.7078	0.4129
Data 203	0.3616	0.6384	0.5665
Data 204	0.3238	0.6762	0.4788
Data 205	0.5491	0.4509	1.2177
Data 206	0.5146	0.4854	1.0603
Data 207	0.5179	0.4829	1.0745
Data 208	0.3829	0.6171	0.6204
Mean	0.4397	0.5604	0.8343
STD	0.0995	0.0995	0.3147

Table 5.2: Results of Frequency Domain Analysis Using Patches and AR Method

## 5.2 Normal Condition (Without Application of Patch)

In this next case, the signals were recorded without any medication under the regular room light. We obtained varying results from subject to subject depending on their stress level. Figures 5.7 and 5.8 show typical examples of parametric and non-parametric PSD estimates for signals recorded under this condition.

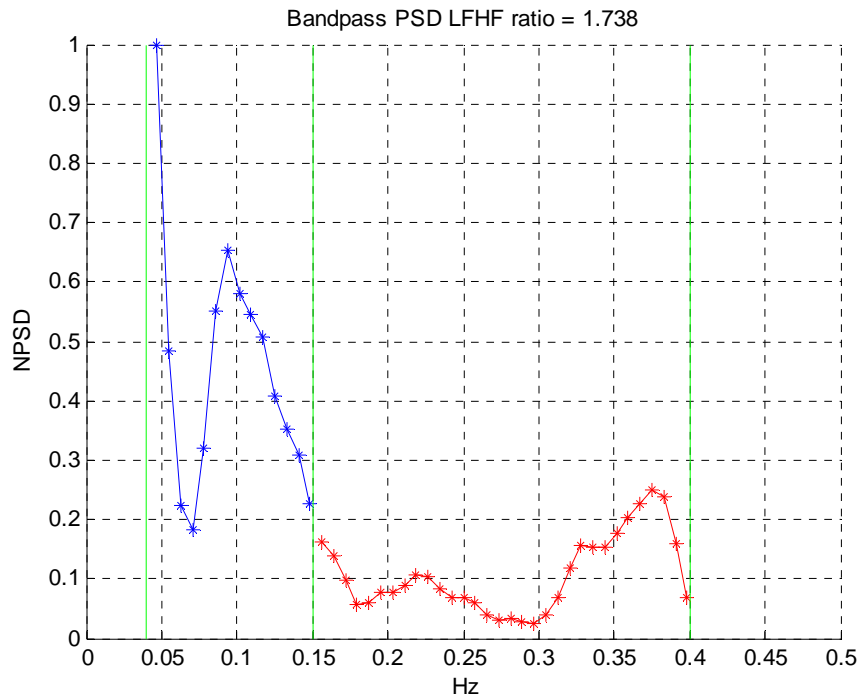


Figure 5.7: Welch Spectrum of a Normal Subject

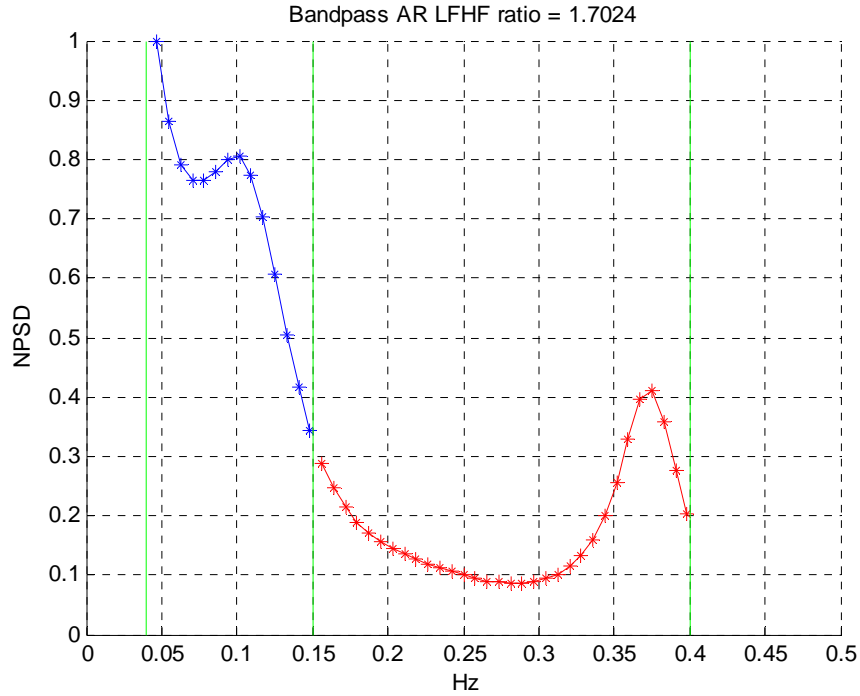


Figure 5.8: AR Spectrum of Normal Subject

Tables 5.3 and 5.4 show results of frequency domain analysis of signals that were recorded under normal (non-medicated) conditions. The results show consistency among the various data records used; however, significantly lower values are obtained for the LF/HF ratio compared to the relaxed (medicated) case. On the average, for these data sets, the LF/HF ratio is approximately twice as high without patch compared to the use of the patch.

Data	LF (n.u)	HF (n.u)	LF/HF
Data 210	0.5815	0.4185	1.3892
Data 211	0.5466	0.4534	1.2056
Data 212	0.7109	0.2891	2.4595
Data 213	0.4014	0.5986	0.6706
Data 214	0.6275	0.3725	1.6846
Data 215	0.5176	0.4824	1.0731
Data 216	0.6418	0.3582	1.7915
Data 217	0.6021	0.3979	1.5132
Data 218	0.6879	0.3121	2.2044
Mean	5908	0.4093	1.5539
STD	0.0943	0.0942	0.5568

Table 5.3: Results of Frequency Domain Analysis of Normal Subject using FFT Method

Data	LF (n.u)	HF (n.u)	LF/HF
Data 210	0.5497	0.4503	1.2208
Data 211	0.5538	0.4462	1.2412
Data 212	0.6593	0.3407	1.9347
Data 213	0.4712	0.5288	0.8911
Data 214	0.6894	0.3106	2.2199
Data 215	0.4975	0.5025	0.99
Data 216	0.6345	0.3655	1.7362
Data 217	0.6103	0.3897	1.566
Data 218	0.6988	0.3012	2.3196
Mean	0.5961	0.4039	1.5688
STD	0.0823	0.0823	0.5211

Table 5.4: Results of Frequency Domain Analysis of Normal Subject using AR Method

### 5.3 Blue Light Effect

We also briefly investigated the effects of blue enriched light on the Autonomic Nervous System. To perform this experiment we used a Go Lite lamp designed by Philips which is expected to enhance the mood and help subjects suffering from Seasonal Affect Disorder (SAD) [27-29]. The Blue light was applied with regular ambient light on test subjects while recording PPG signals. The experimental results in this case were very subjective; on some subjects it tends to have a strong effect while on others it has very mild to no effect. Figures 5.9-5.13 show non-parametric and parametric HRV spectra before and after bringing the blue light into the signal collection environment. The blue light was placed directly in front of the subject's face approximately 3 feet away.



Figure 5.9: Philips Go Lite [33]

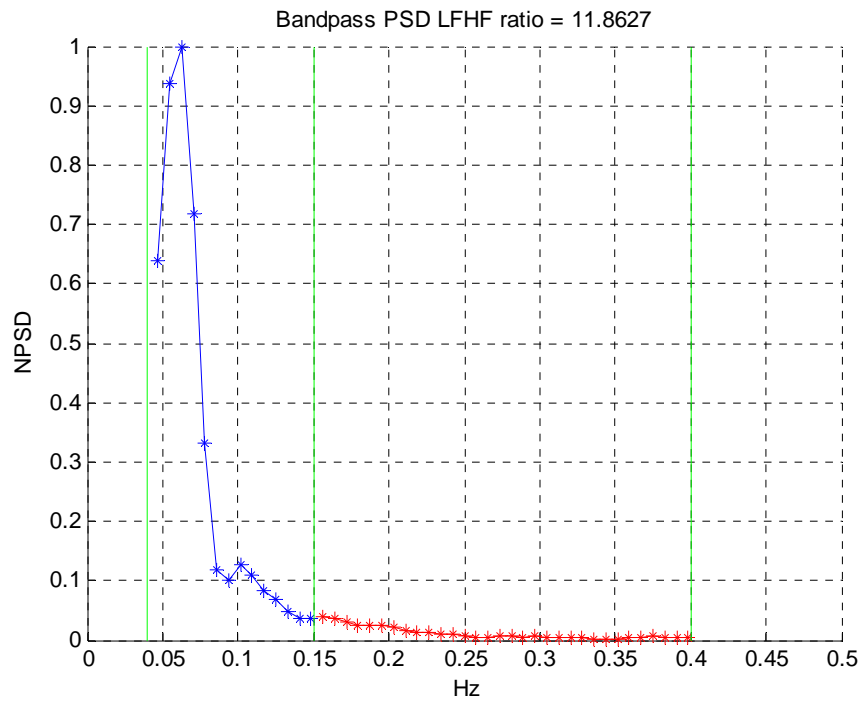


Figure 5.10: Welch Spectrum before Application of Blue Light

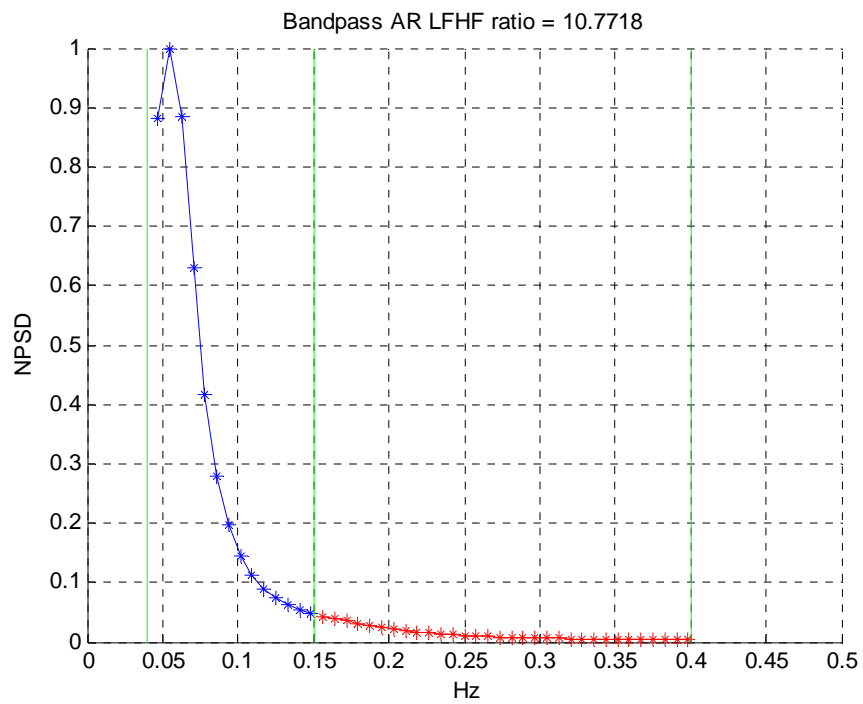


Figure 5.11: AR Spectrum before Application of Blue Light

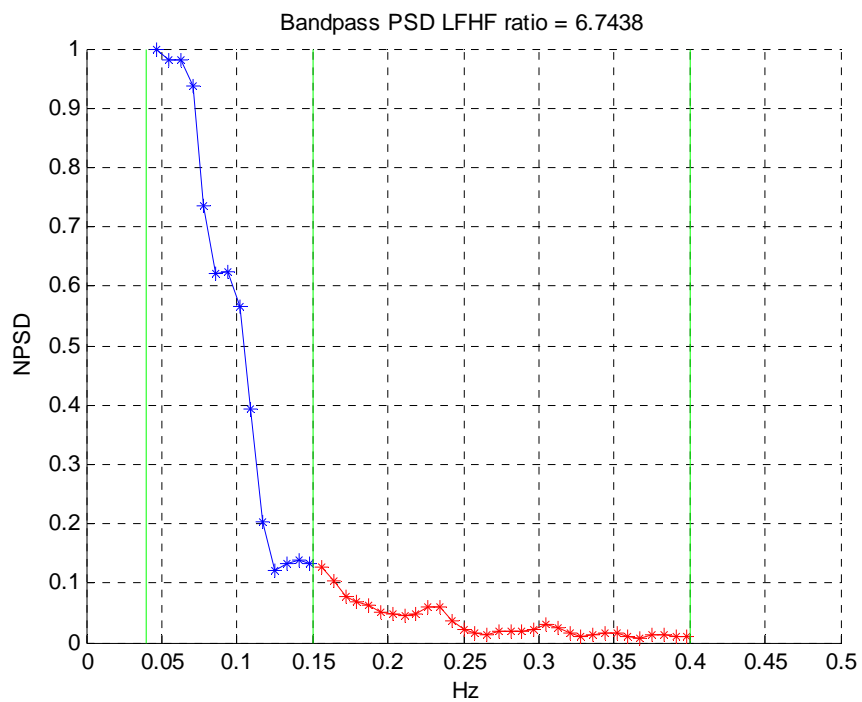


Figure 5.12: Welch Spectrum after Application of Blue Light

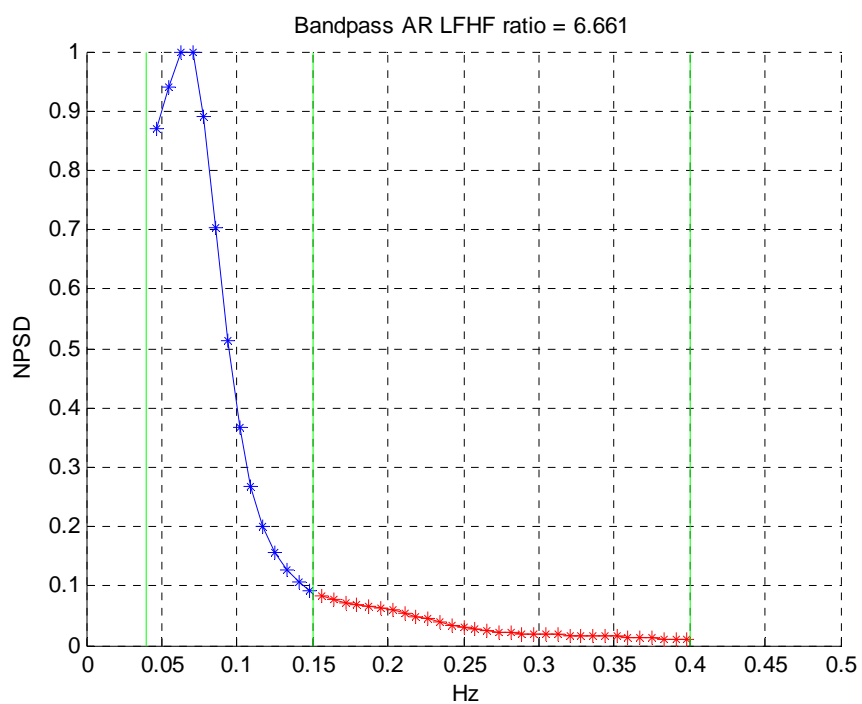


Figure 5.13: AR Spectrum after Application of Blue Light

## **Chapter 6**

### **Advance Techniques, Conclusions and Future Work**

In this chapter we would discuss some advanced processing techniques that could be used for analysis of Heart Rate Variability signals to estimate the balance of the Autonomic Nervous System more accurately. These techniques include a Time Varying Approach and Principal Dynamic Mode method for analyzing HRV signals generated by processing a PPG signal.

#### **6.1 A Time Varying Approach**

The previous frequency domain analysis techniques were the parametric and non-parametric PSD estimation methods. These were used to produce an index that is a marker of balance of the Autonomic Nervous System. The drawback of these techniques is that it produces a single overall index (the LF/HF ratio) that is used as an ANS balance marker. This index does not provide an indication about how the balance of ANS changes over time. This problem is addressed in a time varying approach to spectral analysis where the ANS balance marker i.e. the ratio of power in the low and high frequency region is determined at every instant of time and plotted as function of time. This technique could be advantageous while analyzing a long term HRV signal where knowing the shift in dominance from sympathetic to parasympathetic and vice versa is important.

### 6.1.1 Block Diagram of Time Varying Approach

For performing a time varying analysis we use two 8<sup>th</sup> order IIR Chebyshev Type-I band-pass filters to isolate the contributions of the low and high frequency components of the HRV signal. Exponential averaging was done to produce a smoothed estimate of the power of each of the two output signals so that a time varying LF/HF ratio could be generated. Figure 6.1 shows an overall processing block diagram of the time varying analysis approach to LF/HF ratio calculation.

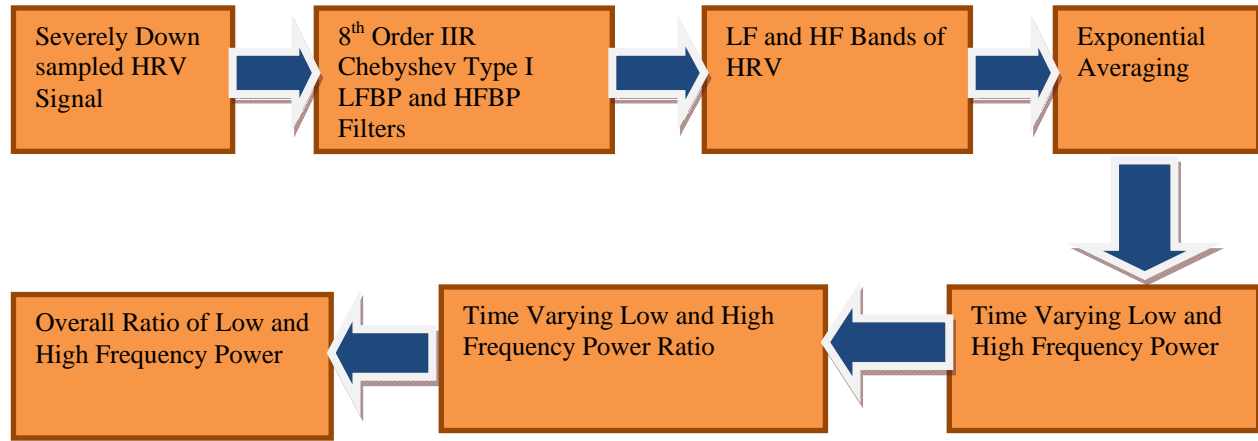


Figure 6.1: Block Diagram of Processing of Time Varying Analysis Technique

Figures 6.2-6.7 are results of step-by-step processing of the above mentioned block diagram. The processing is applied to the severely downsampled HRV signal which is usually chosen as 2 samples/second. In figure 6.5, the first 153 samples or 76.5 secs. belongs to the transient or time-constant interval for data of 5 minutes in duration and this was not considered while computing

$$\text{round}(\log_{10}(1-0.9)/\log_{10}(\alpha\text{Exp}))$$

Where,  $\alpha\text{Exp}$  depends on the length of signal. For example  $\alpha\text{Exp}=0.9851$  gives a time constant of 153 samples so that the step response of the exponential averaging filter is 90% of its maximum value at time index 153.

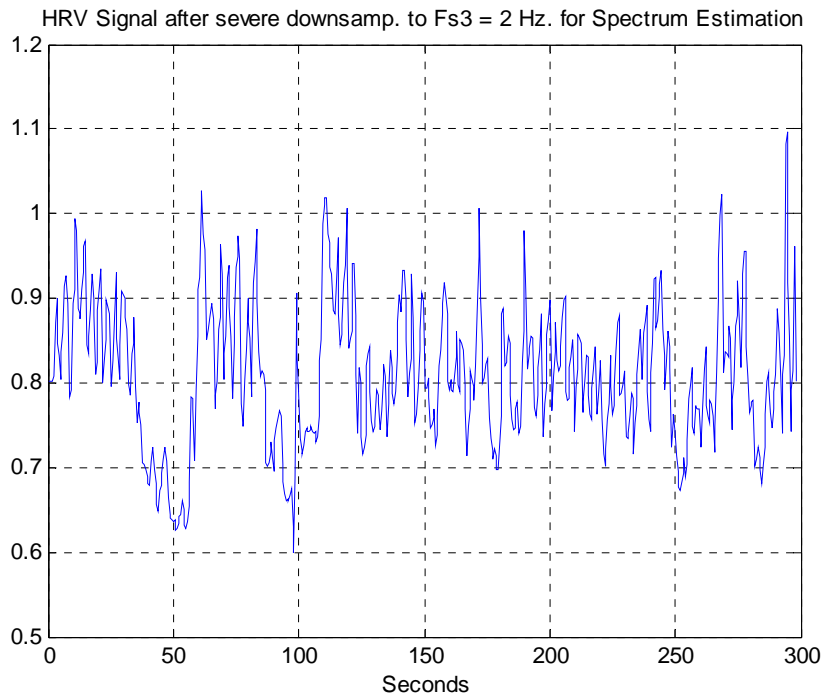


Figure 6.2: HRV Signal after Severe Downsampling

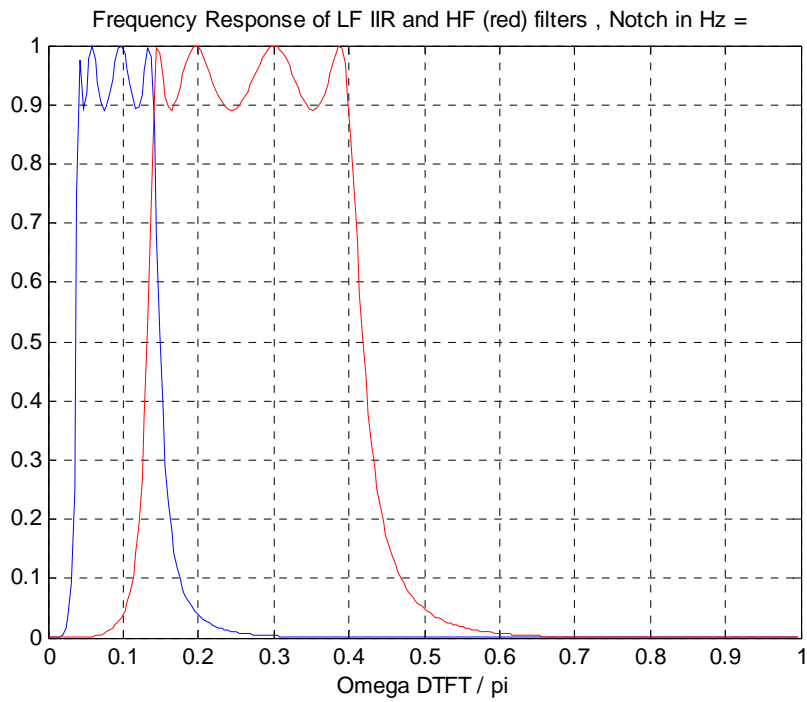


Figure 6.3: Frequency Response of low Frequency and High Frequency IIR Band-Pass Filters

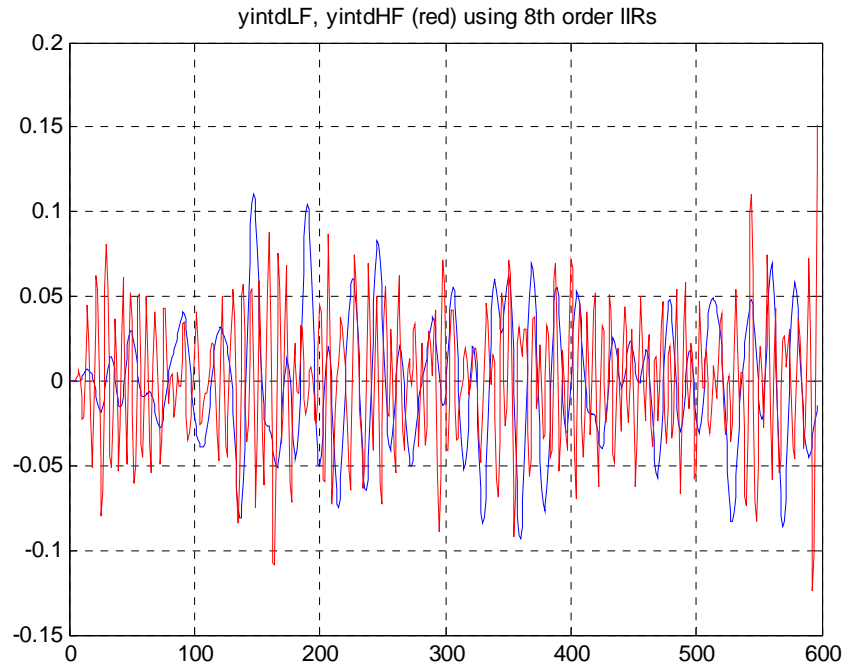


Figure 6.4: Low frequency (Blue) and High Frequency (Red) Bands of HRV signal

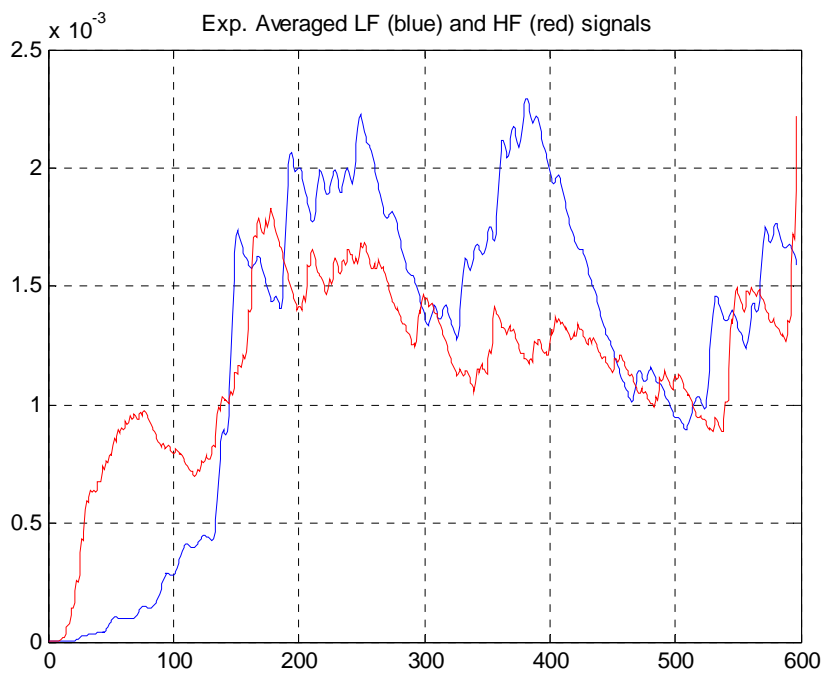


Figure 6.5: Low Frequency (Blue) and High Frequency (Red) HRV signal power as a Function of Time

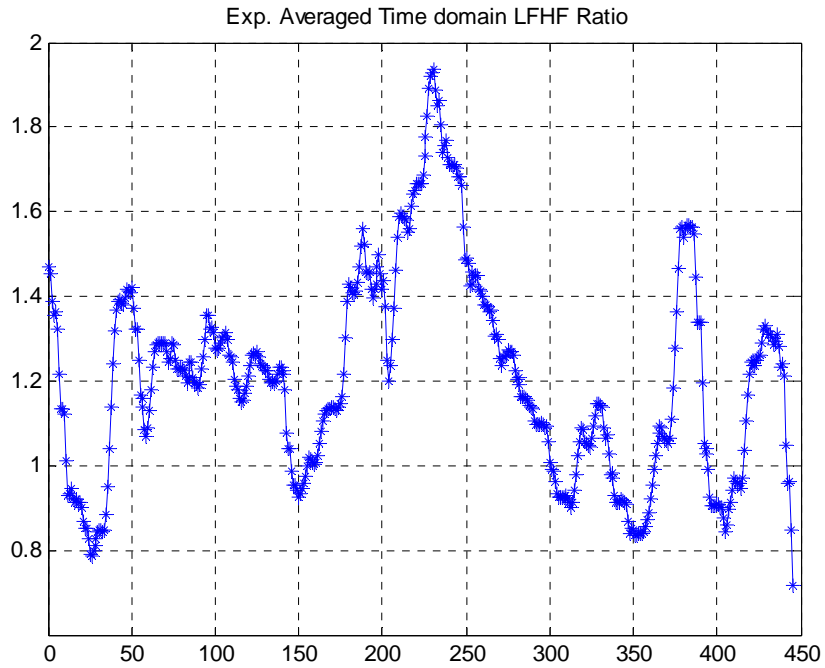


Figure 6.6: Ratio of Low and High Frequency Power as a Function of Time (initial range of the time-constant transient interval is not shown)

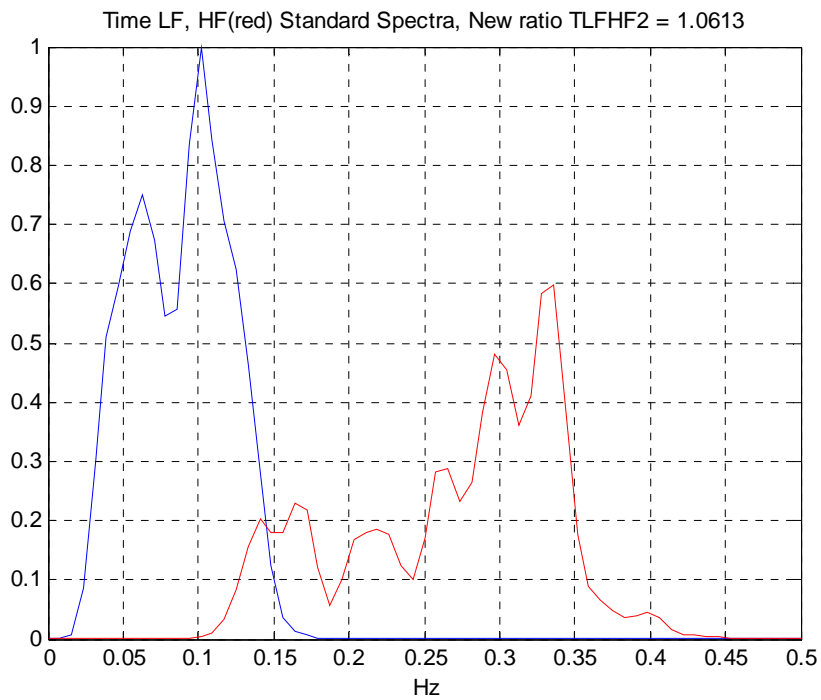


Figure 6.7: Standard Spectra of LF and HF Filter Output Signals Showing Overall Ratio

Also, the overall time varying LF/HF ratio obtained was compared with the ratio obtained using non parametric and parametric PSD estimation techniques and we found these results to be very similar. Table 6.1 shows the comparison of LF/HF ratio obtained using different techniques:

Data	Welch LF/HF	AR LF/HF	TV LF/HF
Data 1	1.61	1.59	1.69
Data 2	1.09	1.08	1
Data 3	2.13	2.13	1.85
Data 4	1.78	1.68	1.84
Data 5	2.23	2.48	1.58
Data 6	0.93	1.1	0.95
Data 7	1.09	1.3	0.96
Data 8	1.08	1.13	0.69
Data 9	1.76	1.81	1.71
Data10	1.39	1.39	1.26
Data11	1.69	1.74	1.79
Data12	2.42	2.18	2.17
Data13	1.02	1.06	0.92
Data14	0.8	0.74	0.65
Data15	0.77	0.74	0.65
Data16	2.4	1.55	2.35
Data17	2.41	2.31	2.59
Data18	1.5	1.5	1.71
Data19	1.64	1.88	1.79
Data20	0.8	0.86	0.95
Mean	1.52	1.51	1.45
STD	0.57	0.57	0.95

Table 6.1: Comparison of Time Varying Ratio (LF/HF) with FFT and AR Based Ratio

### 6.1.2 Verification of Time Varying Analysis Algorithm

To verify the time varying analysis algorithm we generated a signal that was a concatenation of signals from a relaxed subject and stressed subject. The signal was 20 minutes in length divided into segments of relaxed, stressed, relaxed and stressed while each segments being 5 minutes in length. Thus, we expect to see a sudden change in the ratio once we progress from a relaxed-subject segment towards stressed-subject segment and vice versa. The figures 6.8-6.10 shows the HRV signal derived from the concatenated signal and the results confirming marked changes in the low frequency power as well as high frequency power as the analysis progress from one segment to another and therefore a change in the time varying LF/HF ratio. Clearly, all changes are gradual due to the exponential averaging over time.

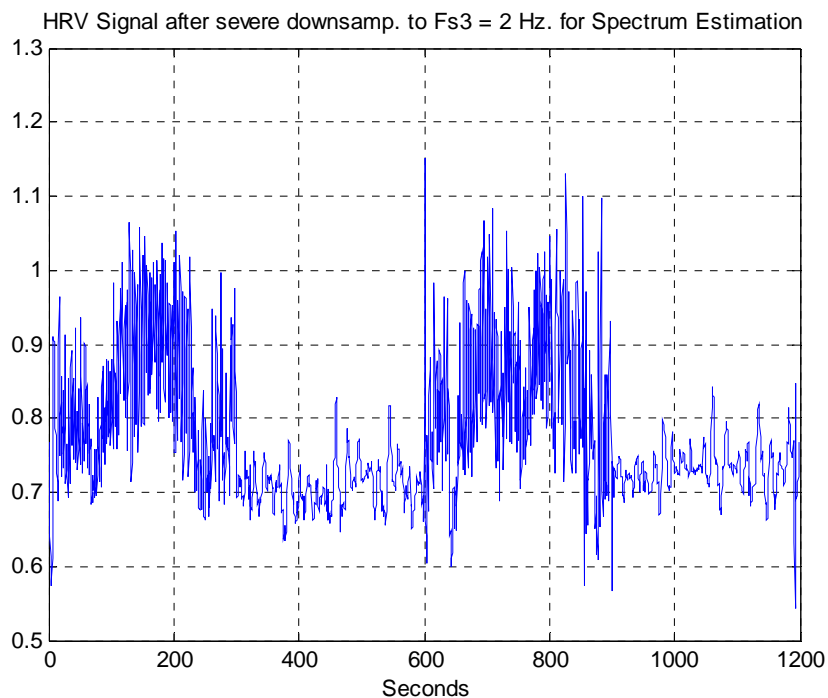


Figure 6.8: Severely Downsampled HRV Signal which is a Combination of Relaxed and Stressed State

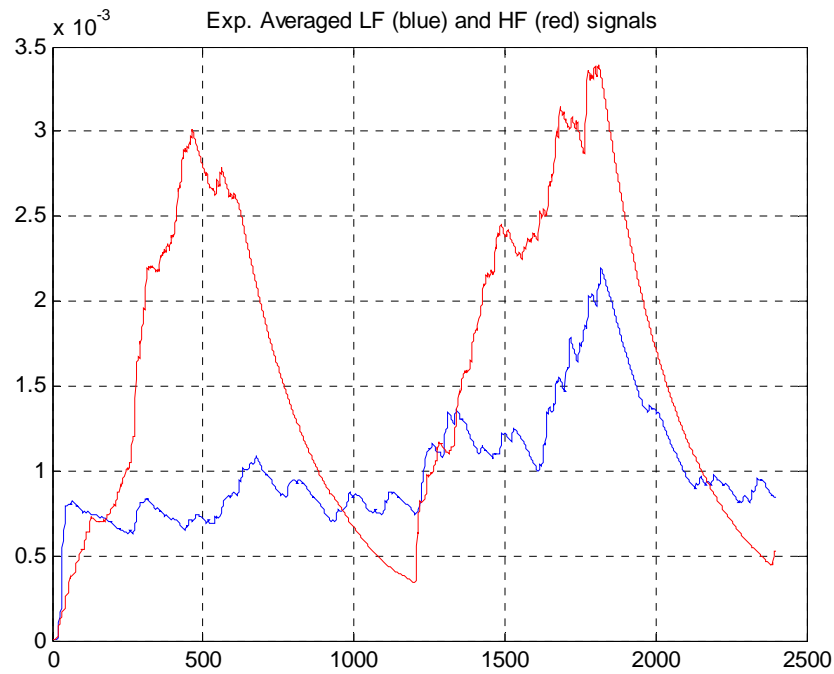


Figure 6.9: Variation in Low Frequency and High Frequency Power as a Function of Time

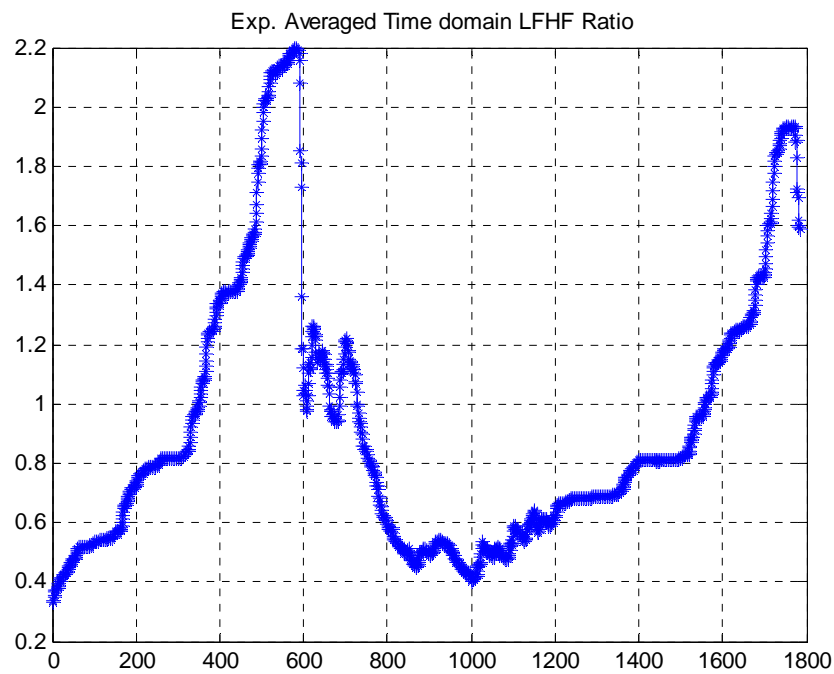


Figure 6.10: Variation in Low Frequency and High Frequency Ratio as a Function of Time

## 6.2 Conclusions

Following are the major conclusions of this thesis:

- A robust algorithm was developed for deriving Heart Rate Variability (HRV) spectra to estimate the balance of Autonomic Nervous System (ANS) (Chapter 3)
- A multiple sensor concept was introduced to overcome noises that get incorporated into a signal due to loss of contact with the sensor. (Chapter 3)
- We showed in chapters 4 and 5 that for a relaxed case (medicated with a nano-scale acupuncture patch) the pNN50 number was high having an average value of 63.18% compared to the normal (un-medicated) case which has an average value of 35.86% and stressed case with mean pNN50 value of 5.46%. Also, we showed that that on an average the LF/HF ratio for the relaxed (medicated) case was lower having a mean value of 0.77 on the FFT spectrum and mean of 0.83 on the AR spectrum compared to normal (un-medicated) which had a mean LF/HF ratio of 1.55 on the FFT spectrum and 1.56 on the AR spectrum.
- Using the results from tables in chapter 4 and 5 a reasonable agreement between time and frequency domain analysis i.e. for low LF/HF ratio, a high pNN50 value is obtained, and vice versa.

In addition, a time varying spectral analysis technique for HRV signals was introduced which would be helpful in estimating the ANS at any particular instant of time. Also, the Time Varying Analysis Technique can detect sudden changes in the shift of dominance from Sympathetic to Parasympathetic Nervous System.

### **6.3 Future Work**

More work remains to be done to develop the multiple sensor PPG signal merging approach. More experimentation to validate various correlations that exist between time and frequency domain analysis is also an important future topic. Finally, using more advance analysis techniques to better estimate the balance of Autonomic Nervous System is an important future research topic. A brief discussion of these future topics follows.

#### **6.3.1 Multiple Sensors Concepts**

We explored the multiple sensors concept and stated that it could well be used as a way to produce an input signal that is free from noises and distortions that arise due to loss of contact, motion artifacts, etc. However, a more sophisticated and automated scheme needs to be designed to generate a signal that is an optimal combination of signals obtained using multiple sensors.

#### **6.3.2 More Experiments**

More experiments need to be done to verify correlation between various time domain and frequency domain parameters. For this research we only incorporated the pNN50 parameter to check the expected correlation with frequency domain markers produced by our algorithm. However, there are other time-domain parameters that could have a correlation with frequency domain parameters and this could be validated empirically

#### **6.3.3 HRV Analysis Using Principal Dynamic Modes**

As mentioned earlier in chapter 2, the physiological mechanism those are responsible for heart rate fluctuations have nonlinear components. Thus, a nonlinear analysis technique could be used

to better estimate the state of the Autonomic Nervous System. HRV analysis using Principal Dynamic Modes (PDMs) seems to address the non-linearity problem associated with the ANS. Therefore, HRV analysis using this method could be used to more accurately estimate the ANS state.

## REFERENCES

- [1]S. Chatlapalli, H. Nazeran, V Melarkod, R Krishnam, E Estrada, Y Pamula, S Cabrera, “Accurate Derivation of Heart Rate Variability Signal for Detection of Sleep Disordered Breathing in Children”, Proceedings of the 26<sup>th</sup> Annual International Conference of the IEEE EMBS San Francisco, CA, USA September 1-5, 2004
- [2]Camm, A. J., et al. "Heart rate variability: standards of measurement, physiological interpretation and clinical use. Task Force of the European Society of Cardiology and the North American Society of Pacing and Electrophysiology." *Circulation* 93.5 (1996): 1043-1065
- [3]M. Bolanos, H. Nazeran and E.Haltiwagner,”Comparison of Heart Rate Variability Signal Features Derived from Electrocardiography and Photoplethysmography in Healthy Individuals, Proceedings of the 28<sup>th</sup> IEEE EMBS Annual International Conference New York City, Aug 30-Sep 3, 2006.
- [4][http://www.polar.com/e\\_manuals/RS800CX/Polar\\_RS800CX\\_user\\_manual\\_English/ch11.html](http://www.polar.com/e_manuals/RS800CX/Polar_RS800CX_user_manual_English/ch11.html)
- [5]A. Petranas, S. Daukantas, V. Marozas, A. Lukosevicius, “Photoplethysmography Based Heart Rate Registration in Rest and Physical Activity”, Conference Biomedical Engineering
- [6]<http://www.biocomtech.com/hrvscientific>
- [7]Autonomic Nervous System at Dorland’s Medical Dictionary
- [8] <http://www.nios.ac.in/media/documents/secscicour/English/Chapter-23.pdf>
- [9]Vanisree K, Jyothi Singaraju, “Automatic Detection of ECG R-R Interval Using Discrete Wavelet Transformation”, International Journal on Computer Science and Engineering.
- [10]<http://a-fib.com/treatments-for-atrial-fibrillation/diagnostic-testing/the-ekg-signal/>
- [11]P. Manimegalai, Ashima Sahoo, K. Thanushkodi, “Wavelet Based Cardiovascular Parameters Estimation System From ECG and PPG Signals” European Journal of Scientific Research ISSN 1450-216X Vol.65 NO.4(2011), pp 453-468
- [12]Autonomic Nervous System at Dorland’s Medical Dictionary
- [13]G.Ranganathan, V. Bindhu, Dr.R.Rangarajan, “Signal Processing of Heart Rate Variability Using Wavelet Transform For Mental Stress Measurement”, Journal of Theoretical and Applied Information Technology.
- [14]Desok Kim, Yunhwan Seo, Jaegeol Cho, Chul-Ho Cho, “Detection of Subjects with Higher Self-Reporting Stress Scores Using Hear Rate Variability Pattern During the Day”, 30<sup>th</sup> Annual

International IEEE EMBS Conference Vancouver, British Columbia, Canada, August 20-24, 2008

[15]<http://physionet.org/physiobank/database/mitdb/>

[16]Yuru Zhong, Hengliang Wong, Ki Hwan Ju, Kung-Ming Jan and Ki H. Chon, “Nonlinear Analysis of the Separate Contributions of Autonomic Nervous Systems to Heart Rate Variability Using Principal Dynamic Modes”, IEEE Transaction on Biomedical Engineering, VOL.51. NO.2, February 2004

[17]Yuru Zhong, Kung-Ming Jan, Ki Hwan Ju and Ki H. Chon,”Quantifying Cardiac Sympathetic and Parasympathetic Nervous Activities Using Principal Dynamic Modes Analysis of Heart Rate Variability”, Am J Physiol Heart Circ Physiol 291: H1475-H1483, 2006

[18]Hsein-Ping Kew, Do-Un Jeong, “Variable Threshold Method for ECG R-Peak Detection”, J Med Syst (2011) 35:1085-1094

[19]Olivia Manfrini, Carmine Pizzi, Davide Trere, Fiorella Fontana, Raffaele Bugiardini,”Parasympathetic failure and risk of subsequent coronary events in unstable angina and non-ST-segment elevation myocardial infarction” European Heart Journal 24, No. 17 (2003): 1560-1566

[20]Hui-Min Wang and Sheng-Chieh Huang, “SDNN/RMSSD as a surrogate for LF/HF: A Revised Investigation”, Hindawai Publishing Corporation Modeling and Simulation in Engineering Volume 2012, Article ID 931943, 8 Pages

[21]Kubios HRV Analysis Software, Version 2.0, Department of Physics, University of Kuopio

[22]Joao Luiz Azevedo de Carvalho, Adson Ferreira da Rocha, Francisco Assis de Oliveira Nascimento, Joao Souza Neto, Luiz Fernando Junqueira Jr,”Development of Matlab Software for Analysis of Heart Rate Variability”

[23]Mika P. Tarvainen, Perttu O. Ranta-aho and Pasi A. Karjalainen,”An Advanced Detrending Method With Application to HRV Analysis”, IEEE Transaction on Biomedical Engineering, VOL 49, NO. 2, FEBRUARY 2002

[24]Vasilis Z. Marmarelis, “Identification of Nonlinear Biological Systems Using Laguerre Expansions of Kernels” Annals of Biomedical Engineering, vol 21, pp 573-589, 1993

[25]Jongyoon Choi and Ricardo Gutierrez-Osuna, “Using Heart Rate Monitors to Detect Mental Stress” 2009 Body Sensor Networks

[26]Jongyoon Choi and Ricardo Gutierrez-Osuna, “Estimating the Principal Dynamic Modes of Autonomic State with Wearable Sensors”, Department of Computer Science, Texas A&M University, Technical Report tamu-cs-tr-2008-7-2

- [27]Sallie Baxendale, John O’Sullivan, Dominic Heaney, “Bright Light Therapy as an Add on Treatment for Medically Intractable Epilepsy”, *Epilepsy and Behavior* 24(2012) 359-364
- [28]M.C.M. Gordijn, D.‘t Mannetje, Y. Meesters, “The Effects of Blue-Enriched Light Treatment Compared to Standard Light Treatment in a Seasonal Affective Disorder”, *Journal of Affective Disorders* 136 (2012) 72-80
- [29]J. van Hoof, A.C. Westerlaken, M.P.J. Aarts, E.J.M. Wouters, A.M.C. Schoutens, M.M. Sinoo and M.B.C. Aries, ”Light Therapy: Methodological Issues From an Engineering Perspective”, *Technology and Health Care* 20 (2012) 11-23
- [30]H. Nazeran, “A Double-blind Placebo-Controlled Heart Rate Variability Investigation to Evaluate the Quantitative Effects of the Life Wave Y-Age Aeon Patch on the Autonomic Nervous System”, *AEON Patch Heart Rate Variability Study Report*.
- [31] <http://acupuncturepatches.com/products/aeon/>
- [32] <http://www.nikigratrixblog.com/shop/physical-product-store/acupressure-patches/y-age-aeon-patch/>
- [33] <http://www.usa.philips.com/c-m-pe/light-therapy/#3>

## **CURRICULUM VITAE**

Ajay Kumar Verma was born in Varanasi, Uttar Pradesh, India on August 29<sup>th</sup> 1988. After completing high school in 2007 he attended Uttar Pradesh Technical University, Lucknow to pursue a Bachelor of Technology Degree in Electronics and Instrumentation Engineering. After obtaining a Bachelor of Technology degree in Electronics and Instrumentation Engineering in 2011 he decided to pursue a master's degree in Electrical Engineering in the Department of Electrical and Computer Engineering at The University of Texas at El Paso. He enrolled as a graduate student in the Department of Electrical and Computer Engineering in spring 2012 Semester. While being a graduate student at UTEP he worked in the Department of Electrical and Computer Engineering, Office of International Programs and Department of Industrial Manufacturing and Systems Engineering as a Research Assistant.

Present Address: 2401 N. Oregon ST.

El Paso, Texas

United States-79902

Permanent Address: Indian Institute of Technology Roorkee

Shivalik Apartments A-102

Roorkee-247667

Uttarakhand, India